Architectural Diversity of Submarine Unconfined Lobate Deposits

Tim R. McHargue[1] (Corresponding author), **David M. Hodgson**[2], and **Eitan Shelef**[3]

[1]*School of Earth, Energy and Environmental Sciences, Department of Geological Sciences, Stanford University, Braun Hall #317, 450 Serra Mall, Building 320, Stanford, CA 94305.*

email: timmchargue@gmail.com

[2]*Stratigraphy Group, School of Earth and Environment, University of Leeds, Leeds LS2 9JT, U.K.* email: D.Hodgson@leeds.ac.uk

[3]*Department of Environmental Sciences, University of Pennsylvania, 310 SRCC, 4107 O'Hara Street, Pittsburgh, PA 15260.* email: shelef@pitt.edu

Key words: submarine, fan, lobe, unconfined, turbidite, debris flow, distributary, channel, seismic, geomorphology

ABSTRACT

The most popular model for submarine unconfined lobate deposits has the following attributes: (1) a single feeder channel that delivers sediment, (2) a set of distributary channels present only in the proximal part of the lobate body, and (3) unchannelized tabular deposits present in the middle and distal part of the lobate deposit. This model has become a standard to guide interpretation of outcrop and subsurface examples of submarine lobate deposits. In this contribution, three well imaged subsurface lobate deposits are described that display three markedly different morphologies, all of which differ from the “standard” model. All three lobate examples are buried by less than 150m of muddy sediment and imaged with high resolution 3D reflection seismic data of similar quality and resolution. Distinctively different distributary channel patterns are present in two of the examples, and no distributaries are imaged in a third example. We conclude that if channels are not imaged, it is because channels are not present. The different distributary channel patterns are interpreted to have resulted from different processes: (1) a lobate deposit that is pervasively channelized by many distributaries that have avulsed from numerous nodes is interpreted to result from mud-rich, stratified, turbulent flows ; (2) an absence of distributaries in a lobate deposit is interpreted to result from collapse of mud-poor, turbulent flows remobilized from littoral drift; and (3) a lobate deposit with only a few, long, straight distributaries without avulsions is interpreted to be dominated by debris flows (laminar flows) . Reconciling 3D seismic morphologies with observations of channels, scours, and amalgamation zones in outcrops is problematic. It is concluded from this study that, when characterizing unconfined deep water deposits, multiple models with significant differences in predicted permeability structure should be considered.

1. INTRODUCTION

Submarine fans and other submarine unconfined lobate deposits are repositories of continentally-derived coarse sediment in the deep sea (e.g. Normark, 1978), and are important archives of palaeoenvironmental change. The potentially large volumes of sand deposited in lobate deposits make them important targets for hydrocarbon exploration and production

(Weimer et al., 2000) as well as potentially important aquifers, or reservoirs for the sequestration of CO2 or hazardous fluids (Ketzer et al., 2005). Simulations of fluid dynamics and volume within this reservoir type designed to optimize performance, either during fluid injection or extraction, necessitate a detailed understanding of depositional architecture, heterogeneity distribution, and permeability structure.

Diverse conceptual models of lobate deposits have been proposed (e.g. Normark, 1970; Mutti and Ricci Lucchi, 1972; Walker, 1978; Stow, 1985, 1986; Redding and Richards, 1994). Tectonic setting, source terrain, transportation mechanisms, and bathymetric irregularities have long been acknowledged to be important when predicting the characteristics of lobate deposits (Normark, 1970; Mutti and Ricci Lucchi, 1972; Stow, 1985, 1986; Redding and Richards, 1994). Early submarine fan models included a diverging set of avulsed channel-levee complexes each of which terminated at the distal end with a sand-rich "depositional lobe" (Normark, 1970; Mutti and Ghibaudo, 1972). Recent studies with more complete or detailed data demonstrate that lobate deposits at the terminus of each distributary channel complex typically consist of multiple smaller, nested or overlapping offset lobate to palmate bodies (e.g. Mutti, 1977; O'Connell et al., 1991; Lowry et al., 1993; Martinsen et al., 2000; Sullivan et al., 2000; Johnson et al., 2001; Gardner et al., 2003; Posamentier and Kolla, 2003; Hodgson et al., 2006; Deptuck et al., 2008: Prélat, et al., 2009; Groenenberg et al., 2010; Mulder and Etienne, 2010; and Prélat and Hodgson, 2013; Picot et al., 2016). Prélat et al. (2009) proposed a hierarchical scheme to account for the observed complexity of lobate deposits and proposed that a Lobe System or Complex Set is composed of smaller Lobe Complexes which in turn are composed of Lobes with smaller constituent Lobe Elements. This hierarchical approach has been adopted by multiple authors in subsequent papers (Prélat, et al., 2010; Groenenberg et al., 2010; Mulder and Etienne, 2010; Grundvåg et al., 2014). However, the application of this model, here referred to as the Prélat Hierarchical Model, is challenging in many cases, including examples where seismic morphology is well imaged, as will be explored in this paper. Also, the hierarchical model requires one to interpret which level within the hierarchy is represented by a lobate unit in order to know which term is appropriate. Unfortunately, the term lobe is used as one of the levels within the hierarchical scheme making it ambiguous for use as a general term for lobate deposits. We are reminded that Normark et al. (1993) lamented that confusion in the use of the term "depositional lobe" is common.

The presence of channels in at least some lobate deposits has long been recognized. Normark (1970), here referred to as the "Standard" Lobe Model, included shallow distributary channels in the proximal portion of his definition of a lobe but few to none in the distal portion of the lobe. Beaubouef et al. (1999), Sullivan et al. (2000), Carr and Gardner (2000), and Gardner et al. (2003), to varying degrees, interpreted the presence of channels across lobate depositional bodies. The recent fan model of Prélat et al. (2009, 2010) does not emphasize distributary channels within depositional lobes. Mulder and Etienne (2010) propose that poorly channelized lobes develop in settings with sand-dominated flows whereas lobes with a distinctive distributary channel network develop in settings with mud-rich flows. The potential presence and distribution of channels within lobate deposits are of particular interest because, relative to the non-channelized portion of a lobate deposit, sand caliber can be coarser, and permeability higher within channels so that channel deposits may be a preferred pathway for subsurface fluids (Pyles et al. 2014; Jones et al., 2015; Hofstra et al., 2016; Bell et al., 2018).

In modern or near modern turbidite systems distributary channels have been imaged within lobes in some cases (O'Connell et al., 1991; Twichell et al., 1992; Kidd, 1999;

Posamentier and Kolla, 2003; Hadler-Jacobson et al., 2005, 2007; Clark and McHargue, 2007; Bourget et al., 2010; Bakke et al., 2013; and Doughty-Jones et al., 2017). However, even in modern submarine fan systems, detailed bathymetric records and sidescan sonar recordings often do not produce clear images of distributary channel networks within lobate deposits (Bonnel, et al., 2005; Gervais et al., 2006; Jegou, et al., 2008; Dennielou et al., 2009; Bourget et al., 2010; Hanquiez et al., 2010; Migeon et al., 2010) even though incisional transient fan channels, when present, may be well imaged (Adeogba et al., 2005: Gamberi and Rovere, 2011; Maier et al., 2011, 2012, 2013; Barton, 2012; Prather et al., 2012a; Yang and Kim, 2014).

Outcrop studies of lobate deposits with laterally extensive exposure have guided concepts of architecture and facies distribution (Mutti and Ricci Lucchi, 1972; Martinsen et al., 2000; Sullivan et al., 2000; Johnson et al., 2001; Gardner et al., 2003; Hodgson et al., 2006; Prélat, et al., 2009; Groenenberg et al., 2010; and Prélat and Hodgson, 2013). However, there are few opportunities to unambiguously document the three-dimensional relationships of architectural components within lobate deposits. Interestingly, these few examples display meaningful differences. The somewhat lobate deposits of the Brushy Canyon Formation are extensively channelized with tabular sands in overbank positions (e.g. Gardner et al., 2003). The Ross Formation displays well developed tabular sandstone units associated with multiple channels (e.g. Martinsen et al., 2000; Sullivan et al., 2000; Pyles and Jennette, 2009; and Pierce et al., 2018). The lobate deposits with the most continuous and extensive exposure are within the Skoorsteenberg Formation in the Tanqua Karoo Basin, South Africa (e.g. Johnson et al., 2001; Hodgson et al., 2006; Prélat, et al., 2009; Groenenberg et al., 2010; and Prélat and Hodgson, 2013). Although lobate units are extensively exposed within the Skoorsteenberg Formation, conventional channels, such as seen in the Ross Formation, are present only in the most proximal exposure of the lobate units (Johnson et al., 2001; Hodgetts et al., 2004; Hodgson et al., 2006). Elsewhere, zones of amalgamation have been interpreted as possible channels arranged in a distributary pattern within palmate depositional units (Johnson et al., 2001; Hodgetts et al., 2004). The Skoorsteenberg Formation outcrops also have been instrumental in providing the basis for a hierarchical arrangement of components within the lobate deposits (Prélat, et al., 2009; Groenenberg et al., 2010; and Prélat and Hodgson, 2013).

In subsurface examples, images of submarine lobate deposits, even in high quality 3D reflection seismic volumes, often reveal few, if any, details of architectural features within or on the surface of the lobate deposits. In some cases, lens-shaped lobate deposits, typically stacked in a compensating pattern (*sensu* Mutti and Sonnino, 1981), can be recognized within a larger lobate system (e.g. Gervais et al., 2006; Saller et al., 2008; Deptuck et al., 2008; Bourget et al., 2010; Prélat et al., 2010; Yang and Kim, 2014), but even these gross features may not be resolved in the deep subsurface. Consequently, more often than not, the presence of distributary channels and other architectural features of lobate deposits are inferred based on a model, or models, about which there is considerable uncertainty.

In order to better guide the characterization of lobate deposits in the subsurface, it is necessary to know what models of lobate deposits have been proposed, what the characteristics of each model are, and what information is available to guide an interpreter to select the most appropriate model or models. Toward this end, we describe three example lobate deposits with fundamentally different architectures. We describe the context within which each lobate deposit is found and suggest possible controlling mechanisms. The shape, distribution, and avulsion pattern of channels, if present, are key criteria for discriminating between these three models as well as from other models such as the “Standard” Lobe Model or the Prélat Hierarchical Model.

2. EXAMPLE 1: A PERVASIVELY CHANNELIZED LOBATE DEPOSIT

2.1 Example 1 Regional Setting

Lobate Example 1 is located on the continental slope of the western Niger Delta. The continental slope in the study area is irregular (stepped profile of Prather et al., 1998; Prather, 2003), including areas of both high and low gradient, as well as ridges that tend to stand above the regional slope profile (Allen, 1965; Doust and Omatsola, 1990; Damuth, 1994; Pirmez et al., 2000; Steffens et al., 2003). The steep segments of the profile are formed on the seaward flanks of basinward verging thrusts cored by over-pressured buoyant mud. The areas of low gradient (steps of Prather et al., 1998) occur on the landward sides of the thrust ridges. Lobate Example 1 accumulated within a sediment wedge on one of these steps in what has been called a slope apron (Gorseline and Emery, 1959; Prather et al., 2012a; Barton, 2012) within healed slope accommodation (Prather, 2000, 2003; Prather et al., 2012a; Barton, 2012, Sylvester et al., 2012).

2.2 Example 1 Seismic Data

Images of Lobate Example 1 (Figures 1 and 2) are derived entirely from industry standard three-dimensional reflection seismic data. The interpreted data have a dominant frequency of about 60 Hz at the shallow depth of the studied lobate deposit, which, assuming an acoustic velocity of 1700 m/sec, provides a nominal vertical resolution of approximately 15 m. Sample spacing is 4ms and bin spacing is 12.5m by 12.5m. Planform images provided in this paper are horizon-referenced displays garnered from the uppermost 150 milliseconds (128m) of data below the seabed. The contiguous seismic volumes that are the primary focus of this study cover an irregularly shaped area of approximately 5500 sq. km. The seismic volumes extend from near the modern shelf edge to a position on the continental slope approximately 110km seaward from the shelf edge. An adjacent studied volume with the same resolution and sample spacing covers about 2000 sq. km. on the middle slope.

2.3 Example 1 Description

Lobate Example 1 (Figures 1 and 2) has been called a lobe in a previous publication and description (Prélat et al., 2010, their Figure 4). They noted that Lobate Example 1 is the youngest of several lobate units. Each lobate unit is displaced eastward of its predecessor, occupying low topography between the mounded sediment of the previous lobate deposit to the west and the regional southwest-dipping slope to the east (Prélat et al., 2010).

Lobate Example 1 is located approximately 95km from the modern shelf edge. It is approximately 14km wide, in excess of 12km long, with a maximum thickness of 130m near the proximal (North) end of the lobe, yielding a width to thickness ratio of 108:1 (Prélat et al., 2010). Lobate Example 1 is buried by approximately 120m to 170m of mud-rich sediments in about 2250m of water in a middle slope position. No core samples are available from Lobate Example 1. Sediment transport generally was from north to south or southwest.

The single feeder channel complex (approximately 600m to 700m wide) avulsed from a much larger parent channel system. A portion of this large parent channel system was previously illustrated though not discussed (southernmost channel system, unnamed, of Jobe et al., 2015, figure 2). The apparent similarity of this parent system to the documented complexity of the adjacent channel system Y (Jobe et al., 2015) suggests a similarly diverse heterolithic fill with multiple episodes of erosion and aggradation. Confinement of the feeder channel complex to Lobate Example 1 was provided by a combination of erosion and outer, or external, levee aggradation (Figures 2A and 2B). Outer levees flanking the feeder channel complex are up to 50m thick and 500m wide, represented in reflection seismic data by low root-mean-squared (RMS) amplitude values (Figure 2A, B). Sediment from the single levee-confined feeder channel complex was dispersed across Lobate Example 1 via a system of distributary channels (each 300m or less in width (Figure 1)). Avulsion nodes are observed at multiple locations within the distributary channel system, including at the proximal head and at numerous locations all across Lobate Example 1 (Figure 1). For approximately 3km down flow from the first, most proximal, avulsion node distributary channels continue to be flanked by small outer levees, although levee height decreases down flow to the south until they are no longer resolvable on seismic profiles (Figure 2C). Fill within these proximal distributary channels, as well as within the feeder channel complex, are recorded as high RMS values.

In a down-flow (southward) direction, each of the levee-confined distributary channels transitions into numerous sub-parallel to slightly diverging smaller channels (100m or less in width) that form a 2km to 3km wide cluster (Figure 1). The channel pattern in each cluster is achieved by increasing the number and frequency of avulsion nodes distally so that a few channels in a proximal position increase distally to a large number of closely spaced channels toward the fringe of Lobate Example 1. Despite the fact that limited vertical resolution results in compositing multiple vertically juxtaposed channels within the same image, the entire lobate unit beyond the limit of levee confinement appears to consist of numerous channel clusters. The axis of each cluster follows a path that is sub-parallel to the axis of adjacent clusters and thus the overlap between adjacent clusters is minimal.

Within Lobate Example 1, depositional lenses have been interpreted (Prélat et al., 2010) and can be identified in at least some seismic profiles in the proximal to middle, high relief portion of Lobate Example 1 (Figures 2C and 2D). Distally, the lenses gradually become flatter and thinner until they can no longer be resolved separately (Figure 2E).

2.4 Example 1 Interpretation

No cores are available to confirm interpretations of sediment caliber and distribution. However, seismic RMS amplitudes provide an objective basis for interpretation (Figures 1 and 2). The diversity of amplitudes suggests that Lobate Example 1 received flows containing a wide range of grain-sizes. The feeder channel complex and proximal distributary channels of Lobate Example 1 are confined primarily by outer levees (Figures 2b and 2c). Low seismic RMS amplitudes in the levees suggest that they are composed dominantly of mud. The presence of mud-rich levees requires that the gravity flows that traversed the channels were density stratified including volumetrically significant mud in the upper portions of the flows. Low seismic RMS amplitudes within outer levees contrast with high seismic RMS amplitudes within the feeder channel complex and within distributary channels of Lobate Example 1. High RMS amplitudes require strong contrasts in impedance and suggest the presence of mixed sand and mud within the channels. Further down flow, where levees are no longer discernable, it is suspected that overbank sediments continue to have higher mud content relative to channel sediments accounting for distinct, well imaged channels.

2.5 Example 1 Discussion

2.5.1 Classification

Lobate Example 1 is pervasively channelized from the proximal to the distal margin, and, although previously called a lobe (Prélat et al., 2010), might be classified as a small submarine fan consisting of channel-levee complexes in a distributary pattern. No unchannelized sheet-like deposit is present at the terminus of each distributary channel; rather each distributary channel avulses to form a channel cluster. Perhaps each channel cluster is analogous to a lobe in this case, or, an unchannelized and unresolved lobe is present at the distal end of each small channel of each channel cluster. The latter option implies a very large number of strongly overlapping, unresolved, small lobes, which we think is unreasonable.

2.5.2 Hierarchy

In planform, avulsion nodes and channel density increase in a down flow direction. This trend might provide a basis for defining a hierarchy within Lobate Example 1. The Prélat Hierarchical Model is based on abrupt lateral displacements of sedimentation due to avulsion and Lobate Example 1 has many avulsion nodes. In fact, the high number of avulsion nodes could imply a large and unwieldy number of subordinate hierarchy levels within the deposit, several more levels than accommodated in the Prélat Hierarchical Model. A tendency for the most distal distributary channels to cluster with minimal overlap suggests compensational (lateral offset) stacking of the clusters. So perhaps each cluster represents a lobate subunit in the hierarchy. Unfortunately, although this approach seems attractive, a channel cluster does not resemble a lobe element, or any other level of hierarchy, as described by Prélat et al. (2009, 2010).

Alternatively, perhaps it is inappropriate to impose a hierarchical structure on Lobate Example 1. Straub and Pyles (2012) provided a mechanism for testing hierarchical versus fractal structure with a modified compensational index. Unfortunately, determination of a modified compensational index requires measurement of the thickness of all units but the vertical resolution of the seismic profiles (Figure 2) of Lobate Example 1 is inadequate for this purpose. Nevertheless, qualitatively, channel distribution patterns in Lobe 1 suggest a fractal structure.

Smaller channels in a fractal structure must be smaller in both thickness and width with proportionally smaller compensational offsets. Arguably, this may be the case, as displayed in Figure 1, but cannot be confirmed.

2.5.3 Process

A large channel system with mixed erosion and levee confinement strongly suggests that associated flows contained both sand and abundant mud. Abundant mud in overbank settings further supports the presence of abundant mud in the flows that reached Lobate Example 1. Effective partitioning of sand within channels and mud in overbank positions indicates that the contributing flows were density stratified. As each turbidity current crossed Lobate Example 1, the top of the dilute layer was eventually lost overbank as levee height decreased down flow.

2.6 Summary

In summary, Lobate Example 1 is interpreted to have a well-developed distributary channel system that is reasonably interpreted to display the following characteristics:

(1) Sediments, presumably fluvial/deltaic sediments, were delivered to Lobate Example 1 through a single leveed feeder channel complex that avulsed from an observed large trunk channel system.

(2) Delivered sediments were heterolithic, comprising mud and sand (and gravel?);

(3) Sediments were dispersed across Lobate Example 1 via distributary channels;

(4) The proximal distributary channels were levee confined;

(5) Lobate Example 1 grew as a result of avulsions or bifurcations at numerous and diverse positions along the distributary channel pathways;

(6) The most distal visible channels form channel clusters that stacked relative to one another in a compensational pattern.

(7) Unchannelized tabular deposits are not imaged at the distal ends of the distributary channels or the channel clusters.

(8) This lobate deposit does not conform to prevailing definitions of either a fan or a lobe.

3. EXAMPLE 2: A LOBATE DEPOSIT WITHOUT DISTRIBUTARY CHANNELS

3.1 Example 2 Regional Setting

Lobate Example 2 is located on the continental slope of the Niger Delta (Figures 3-6), approximately 45km from the modern shelf edge, and 70km southeast of example 1. Lobate Example 2 is in an area of relatively low gradient along an irregular stepped profile resulting from deep seated thrusts modified by diapiric deformation of buoyant shales (circular features near the head of Lobate Example 2 in Figure 5) (Allen, 1965; Doust and Omatsola, 1990; Damuth, 1994; Pirmez et al., 2000; Steffens et al., 2003). Lobate Example 2 accumulated within a slope apron (Gorseline and Emery, 1959; Prather et al., 2012a; Barton, 2012) within healed slope accommodation (Prather, 2000, 2003; Prather et al., 2012a; Barton, 2012, Sylvester et al., 2012).

3.2 Example 2 Seismic Data

Images of Lobate Example 2 are derived entirely from industry standard three-dimensional reflection seismic data of very similar vintage and quality to the data that are illustrated for Lobate Example 1. About 6000 sq. km of contiguous 3D reflection seismic data are available in the area around Lobate Example 2 (Figure 3) including the outermost shelf and shelf edge near Lobate Example 2 as well as surrounding slope features. As with Example 1, these interpreted data have a dominant frequency of about 60 Hz at the shallow depth of the studied lobate deposit, which, assuming an acoustic velocity of 1700 m/sec., provides a nominal vertical resolution of approximately 15m. Sample spacing is 4ms and bin spacing is 12.5m by 12.5m. The plan view images provided in this paper for Lobate Example 2 are horizon-referenced displays of data between 50 and 150 milliseconds (42 to128m) below the seabed.

3.3 Example 2 Description

Lobate Example 2 is approximately 6km wide, 14km long, and a maximum of 20m thick (width to thickness ratio of 300:1). Example 2 is buried at approximately 47m below the seabed in 1275m of water in a middle slope position. No core samples are available from Lobate Example 2.

Lobate Example 2 is a high amplitude feature (HAF) displayed in the RMS extractions of Figures 3 through 6 as a light colored object. Several HAFs of diverse sizes and shapes are displayed on the continental slope surrounding Lobate Example 2 including narrow linear HAFs, fan-shaped HAFs, and irregular broad HAFs.

In the area north and east of Lobate Example 2, the shelf edge has a generally smooth to slightly irregular northwest trend (Figure 3). No submarine canyon is imaged at or near the shelf edge. Instead, the shelf edge occasionally is offset landward by approximately 2km by 5-8km wide arcuate indentations (Figure 3). Numerous narrow and linear HAFs are imaged immediately basinward of the arcuate indentations (area X in Figure 3). Some of the linear HAFs appear to terminate down slope, after 5 to 10km or less, in small divergent, fan shaped HAFs that are only one or two kilometers wide and long (area X, Figure 3). Others continue farther down slope and are focused by bathymetry into larger HAFs with stronger amplitudes.

Directly up slope from Lobate Example 2, the shelf edge is beyond the limit of the seismic volume (Figures 3 and 4). In the most proximal portion of the seismic volume numerous linear gullies each give way down slope to a wedge-shaped HAF consisting of a divergent collection of sharp to diffuse linear forms with elevated amplitude (area Y, Figures 3 and 4). The wedge-shaped HAFs overlap to form an apron (sensu Redding and Richards, 1994). After crossing a zone of down-to-the-basin normal faults farther down slope, the apron of wedge-shaped HAFs merges into a single large HAF (area Z, Figure 4). Specific features within the HAF are indistinct although amplitude variations are elongate and define a textural trend that is parallel to the local direction of maximum gradient on the slope. The HAF narrows down slope until it is funneled through two adjacent narrow bathymetric lows to emerge and form the single large HAF of Lobate Example 2 (Figures 4 and 5).

Sediment was supplied to Lobate Example 2 through multiple entry points rather than through a single channel complex (Figures 4 and 5). No outer levees are observed anywhere along the transport path to or within Lobate Example 2. Sediment was dispersed across Lobate Example 2 without leaving any evidence for either avulsions or a distributary channel system (Figure 5). Instead, ill-defined elongate textures are imaged in RMS amplitude extractions in Lobate Example 2 that vary in morphology in planform from lenticular or irregularly shaped to continuous with slightly convergent or slightly divergent margins (Figure 5). The most continuous elongate features lack the sharply defined parallel margins that are clearly imaged in Lobate Example 1 (Figure 1). In cross-section, Lobate Example 2 is tabular and thin (Figure 6) and distinct internal lens shapes, if present, are not resolved with available data.

At the down-flow terminus of Lobate Example 2, deeply incised channels are observed (Figures 5 and 6). One is located at the terminus of the main part of example 2 while another is located at the terminus of a narrow arm of the HAF located to the west of the main body. These deeply incised channels are located at positions that would have, in combination, received any flows and transported sediments that bypassed Lobate Example 2. These incised channels deepen along their path to the southwest (Figure 6) and converge with other erosional channels that follow a basinward course across a bathymetric saddle between two prominent structurally sustained highs (Figure 3).

3.4 Example 2 Interpretation

Much can be inferred regarding the nature of the shelf edge and slope from the regional horizon-based RMS amplitude extraction (Figure 3). The sizes, shapes and linkages of the HAFs displayed on the continental slope indicate the locations of sediment transport paths and deposition. The presence of high amplitudes (light colors in Figures 3-5) within the HAFs is taken as evidence of the deposition of sand-rich sediments within the HAFs.

In the area north and east of Lobate Example 2, no submarine canyon is imaged at or near the shelf edge. Instead, arcuate indentations in the shelf edge are well imaged and are interpreted as coalesced slide scars (Figure 3), which indicates that submarine canyons, if present, also would be imaged. . The narrow and linear HAFs immediately down slope of the slide scars (area X in Figure 3) are interpreted to represent numerous slope gullies terminating in small fan-shaped deposits. The presence of high amplitudes within the gullies is taken as evidence of transport and deposition of sand caliber sediments. Because of the spatial association of slide scars and the gulley clusters (Figure 3), it is inferred that the slide scars were integral to intercepting sand rich shelf sediments and directing them down slope within density currents. The gullies in area Y (Figures 3 and 4) up slope of Lobate Example 2 have the same morphology and clustering as in area X and are inferred to have the same origin as those in area X. Therefore, features in area Y are interpreted to represent the transport path of shelf sands that were intercepted at slide scars and directed through multiple HAPs to Lobate Example 2.

Based on the distribution of high amplitudes across about 45km of the continental slope we interpret that sediment was delivered to Lobate Example 2 from a large number of broadly distributed small point sources (a line source) along the shelf edge rather than from a submarine canyon. The presence of large slide scars suggest that debrites may have contributed to the material that accumulated within Lobate Example 2. However, we speculate that the dominant source of sediment was from littoral drift. The Niger Delta is a wave-dominated system today (Allen, 1965; Doust and Omatsola, 1990) with strong littoral cells (Burke, 1972; Biscara et al., 2013). Because littoral drift potentially is available all along the lowstand delta front, especially concentrated where slumping has intersected the shelf edge, it seems reasonable that gravity flows, consisting of sand-rich littoral deposits, could have spilled over the indented lowstand shelf edge to produce gullies and associated HAFs. The morphology of the HAFs is compatible with having been sourced by very sand-rich littoral drift. High amplitudes strongly suggest the presence of sand within the HAFs and Lobate Example 2. Also, no constructional levees are observable anywhere within Lobate Example 2 or along the train of HAFs leading to Lobate Example 2. These features suggest that the gravity flows that traversed the HAFs to Lobate

Example 2 lacked sufficient mud caliber sediments with which to build levees. Furthermore, these observations support the contention that the HAFs contain sand-rich sediment that originated as littoral drift.

The sediment that was delivered through multiple pathways was dispersed across Lobate Example 2 without leaving any evidence for either avulsions or a distributary channel system (Figure 5). No conventional channels with parallel margins are observed. Instead, ill-defined elongate RMS amplitude textures within Lobate Example 2 (Figure 5) may represent either thickness variations such as might be associated with erosional scours or grain size changes perhaps related to depositional bar forms. Successful imaging of these elongate textures indicates that distributary channels, if present, also would be imaged. Therefore, the absence of imaged distributary channels is attributed not to poor image quality but to the absence of distributary channels.

Some of the most continuous elongate features are slightly darker (lower RMS amplitude) than the surrounding deposits. We interpret this amplitude distribution to result from thinning of the sand-prone deposits within the linear features as a result of scour (reminiscent of the central feature of the Navy Fan (Carvajal et al., 2017)). We further suggest that these elongate features served as the axes of flows and the focus of sediment transport. Successful imaging of these elongate textures indicates that distributary channels, if present, also would be imaged.

Deeply incised channels at the terminus of Lobate Example 2 deepen along their path to the southwest (Figure 6) and converge with other erosional channels (Figure 3). The strongly erosive character of these channels indicates that significant volumes of sediment bypassed

Lobate Example 2, at least at times (Adeogba et al. 2005; Gamberi and Rovere, 2011; Maier et al., 2011, 2012, 2013; Barton, 2012; Prather et al., 2012; Yang and Kim, 2014).

3.5 Example 2 Discussion

3.5.1 Hierarchy

Due to the absence of distributary channels and avulsions, the conventional basis for recognizing smaller hierarchical units within Lobate Example 2 is lacking. Alternatively, because sediments enter Lobate Example 2 from multiple points (two entry points dominate) the deposits derived from each entry point might form subunits within Lobate Example 2. This approach would be most effective if the entry points were active at different times rather than simultaneously. However, thin (meter scale) laterally offset lobe elements within nearby lobe X (Prather et al., 2012a; Jobe et al., 2017) have been confirmed with multiple cores. Comparable lobe elements, if present in Lobate Example 2, are too thin to image with our available data.

3.5.2 Process

The transportation pathway from the shelf to Lobate Example 2 is indicated in seismic data by a trail of high RMS amplitude features. .

Shelf edge slide scars are interpreted to have captured littoral sediment, and generated sand-rich flows with limited density stratification. These flows reached Lobate Example 2 through gullies without levee construction. Assuming that imaging accurately reflects architecture, no distributary channel network is present within Example 2. Variations in RMS amplitude within Example 2 are attributed primarily to variations in thickness resulting from competing combinations of deposition and erosion. Relatively low RMS amplitude linear features are interpreted to represent flow axes that were subject to scour, at least periodically, but not avulsion. We reconcile these observations with the interpretation of sand-rich flows by speculating that deposition of Lobate Example 2 occurred as flows slowed and collapsed at an area of relatively low gradient. Local erosion of linear troughs resulted from flows that had sufficient momentum to scour and bypass Lobate Example 2.

3.5.3 Summary

Lobate Example 2 is interpreted to have no distributary channel system; rather it is reasonably interpreted to display, the following characteristics:

(1) Lobate Example 2 is constructed of sediments derived from multiple points along the shelf edge (a line source) without evidence of a submarine canyon;

(2) The line source is interpreted to reflect capture of littoral drift at slump scar troughs and remobilization across the upper slope;

(3) The delivered sediments are transported from the shelf edge via multiple pathways that are focused by slope topography toward the location of Lobate Example 2;

(4) No resolvable levees are observed anywhere along the transport pathway leading to, or within, Lobate Example 2 suggesting that the turbidity currents that delivered sediments to Lobate Example 2 were extremely sand-rich and that the upper dilute portions of these flows were thin;

(5) No distributary channel system or avulsion nodes are visible within Lobate Example 2 which is interpreted to mean that no channels or avulsion nodes are present.

(6) Deposition is interpreted to result from collapse of sand-rich flows. Other, more robust flows scoured the deposits and bypassed Lobate Example 2.

4. EXAMPLE 3: A CHANNELIZED LOBATE DEPOSIT WITH FEW AVULSIONS

4.1 Example 3 Regional Setting

Lobate Example 3 (Figure 7) is located at the base of slope at a water depth of about 2000m east of Kalimantan, Indonesia, in the Kutei Basin, Makassar Strait. Lobate Example 3 is part of a larger fan system on the basin floor, approximately 40km from the shelf edge (Saller et al., 2008). The continental slope proximal to the fan that contains Lobate Example 3 is irregular, including areas of both high and low gradient, as well as ridges that tend to stand above the regional slope profile. The stepped slope profile results from prominent toe thrusts which maintain a gradient of 2.1^{o} at the base of slope compared to the basin floor gradient of 0.3 ^{o} (Saller et al., 2004).

The fan, including Lobate Example 3, has been imaged and interpreted multiple times (Posamenier et al., 2000; Fowler et al., 2001; Posamentier and Kolla, 2003; Saller et al., 2003, 2004, 2008 and 2010; and Ruzuar et al., 2005). The fan was deposited in association with a sea level lowstand about 240 thousand years ago (Saller et al., 2004). The submarine fan was both preceded and followed immediately by substantial mass transport deposits (Posamenier et al., 2000; Fowler et al., 2001; Posamentier and Kolla, 2003; Saller et al., 2003, 2004, 2008 and 2010; and Ruzuar et al., 2005).

Lobate Example 3 (Figures 7 and 8) is located at approximately a mid-progradation position within a strongly progradational and moderately aggradational succession of lobate bodies (Saller et al., 2008). Each lobe was connected to a channel-levee complex that lengthened as successive lobate deposits were abandoned during progradation. The youngest expression of the channel-levee complex culminated with a terminal lobe (Posamentier et al., 2000; Fowler et al., 2001; Posamentier and Kolla, 2003; Saller et al., 2003, 2004, 2008 and 2010; and Ruzuar et al., 2005). At least one mass transport complex was deposited within the fan during progradation (Posamentier and Kolla, 2003; Saller et al., 2008) and erosion by a younger MTD removed the southern edge of Lobate Example 3.

4.2 Example 3 Seismic Data

Images of Lobate Example 3 are derived entirely from industry standard three-dimensional reflection seismic data acquired in 1998-1999 by WesternGeco as part of the much larger Makassar 3-D survey. The interpreted data have a dominant frequency of about 50 Hz (Saller et al., 2008) at the shallow depth of the studied fan. Assuming an acoustic velocity of 1700 m/sec, the nominal vertical resolution of these data is approximately 17 m. The plan view image provided in this paper is a horizon-referenced RMS amplitude display garnered from the uppermost 200 milliseconds (170m) of data below the seabed. Bin spacing is 12.5m by 12.5m. The studied portion of the seismic volume extends from near the modern base of slope to a position approximately 22km to the east on the basin floor.

4.3 Example 3 Description

Lobate Example 3 is approximately 7km wide, more than 7km long, and a maximum of approximately 43m thick near the proximal (Northwestern) end of the lobate deposits of Example 3, yielding a width to thickness ratio of 163:1 (Figures 7 and 8). Example 3 is buried by approximately 160m of mud-rich sediments in about 2000m of water (Saller et al., 2008). No core samples are available from Lobate Example 3. Sediment transport generally was from northwest to southeast.

At the time of deposition, Lobate Example 3 may have been a terminal lobe of the submarine fan (Posamentier and Kolla, 2003, their frontal splay). Alternatively, its single feeder channel complex (approximately 300m to 500m wide) may have avulsed from a much larger parent channel complex that extended into the basin as the fan prograded. Confinement of the parent channel complex was provided by a 110m thick and 4000m wide outer levee (estimated from Posamentier and Kolla, 2003). The dimensions of the levee, if present, at the time of Lobate Example 3 deposition are unknown.

The single feeder channel complex is about 2 km long between its connection to the larger parent channel complex and the apex of Lobate Example 3. The feeder complex appears to have been confined primarily by erosion although a contemporaneous levee cannot be discounted. Within the feeder channel, which is almost linear, smaller low sinuosity channel elements (sensu McHargue et al., 2011) are distinctly imaged. An avulsion node is present at the distal end of the feeder channel marking the proximal end of a small number of long distributary channels (up to 5km long and 100-300m wide) with very low sinuosity (Figure 7). No other avulsion nodes are recognized within Lobate Example 3. No finer scale channel forms are recognizable surrounding the distributary channels at the distal end of the distributaries. Fill within the distributary channels is too thin to image distinctly in cross-section (Figure 8).

Except for the few distributary channels, imaging of the sediment within Lobate Example 3 ranges from featureless to nodular (Figure 7). The nodules are particularly prominent around the fringe of Lobate Example 3, but subtle variation within the main part of the lobate unit suggests that the nodular texture may be present throughout Example 3. Individual nodules can be up to 200m wide although a full range of smaller sizes, down to the resolution limit of the data, are evident.

In cross-section (Figure 8), Lobate Example 3 is markedly lenticular. It overlies multiple older lenticular lobate units and, at its distal part, is overlain by at least one lobate unit before burial by the channel-levee complex. The sediment within Example 3 is crudely layered and imaged with moderate amplitudes. Compensational stacking of the successive older and younger lobate lenses is evident surrounding the proximal part of Lobate Example 3 (Figure 8, sections A and B) but becomes more subtle distally as lens relief decreases (Figure 8, section C).

4.4 Example 3 Interpretation

No cores are available to confirm interpretations of sediment caliber and distribution. However, the nodular texture of seismic RMS amplitudes, best displayed in planform (Figure 7), provide an objective basis for interpreting the presence of abundant debris flow material. The nodules in this distinct texture are interpreted to be rafted coherent to semi-coherent blocks of allocthonous sediment within a surrounding mass of mud-rich sediment. Lobate Example 3 is crudely layered in cross-section (Figure 8) suggesting that multiple events are present within the lobate unit. The number of events comprising Lobate Example 3 is unknown and it is possible that some events are thinner than can be resolved with available data. The small number of distributary channels within Lobate Example 3, suggests that the lobate unit is composed of at least as many flow events as there are detectable channels, although there could be many more. The fact that distributary channels and small nodular features are imaged suggests that secondary distributaries, if present, would be recognized in these data. The extremely low sinuosity of the erosional feeder and distributary channels of Example 3 are compatible with an interpretation that the channels were eroded by laminar flow events.

Deposits from turbidity currents also may be present within Lobate Example 3. Smaller channel elements with low sinuosity within the feeder channel suggest that turbulent flows may have modified the complex fill of the feeder channel. However, the nodular texture of the lobate deposits strongly suggests that debris flow deposits are present in volumes sufficient to dominate the seismic imaging.

4.5 Example 3 Discussion

4.5.1 Hierarchy

Within the feeder channel of Lobate Example 3, smaller channel forms are visible in plan view (Figure 7). Their presence is compatible with a potential hierarchy (e.g. Campion et al., 2000; Navarre et al., 2002; Sprague et al., 2002, 2005; Gardner et al., 2003; McHargue et al. 2011). However, the smaller channels within the feeder cannot be traced confidently onto the lobate deposit of Lobate Example 3. The only recognized avulsion node of Lobate Example 3 is located at the mouth of the feeder channel (Figure 7). The distributaries that diverge from that avulsion node might provide a basis for defining a hierarchy within Lobate Example 3 (Prélat et al., 2009, 2010). If a separate lens of sediment is associated with each distributary, they would support the possible presence of sub-units within Lobate Example 3. However, no internal lenses are identified unambiguously in cross-section (Figure 8) perhaps due to limited vertical resolution. Also, the absence of secondary distributaries precludes recognition of separate subordinate lobate units in plan view (Figure 7). Determination of a modified compensational index (Straub and Pyles, 2012) requires measurement of the thickness of all units but vertical resolution of the seismic profiles (Figure 8) is inadequate for this purpose. Consequently, the presence of an internal hierarchy within Lobate Example 3 remains speculative.

4.5.2 Process

The absence of secondary avulsion nodes and secondary distributaries coupled with the very low sinuosity of the primary distributaries is distinctive. The widespread nodular texture within Lobate Example 3 deposits is interpreted to represent rafted blocks of material transport by matrix strength of debris flows. The low sinuosity of the erosive feeder channel and distributary channels is consistent with momentum dominated, laminar flow of the debris flows. Also, the relatively high viscosity of debris flows is consistent with the absence of avulsions and secondary distributaries of Lobate Example 3. Therefore, we conclude that Lobate Example 3 is dominated by multiple mass transport deposits and each primary distributary represents one or more episodes of mass flow dominated flows.

Alfaro and Holz (2014, their Figure 19) illustrated a lobate feature with similar characteristics; few avulsion nodes, straight long channels (including "linear scours"), and nodular texture. The deposits of this lobate feature on the Caribbean margin of Colombia are interpreted to consist of mixed slumps, debrites and turbidites, consistent with our interpretation of Lobate Example 3. Visually similar elongate non-avulsing features have been produced in physical experiments (Fernandez et al., 2014) to result from laminar, or, at most, weakly turbulent flows.

4.5.3 Summary

Lobate Example 3 is interpreted to have a small number of straight distributary channels, and is reasonably interpreted to display, the following characteristics:

(1) Lobate Example 3 is one of several lobate features within a submarine fan that evolved into a levee confined channel complex with a terminal lobe;

(2) Sediments were delivered to Lobate Example 3 via a straight, erosional conduit without discernable levees and included minor slightly sinuous channel elements within its fill;

(3) Lobate Example 3 displays a prominent nodular texture in plan view with individual nodules up to 200m wide;

(4) A few, straight distributary channels are visible within Lobate Example 3 although no secondary distributaries are observed;

(5) Only one avulsion node is observed located at the mouth of the feeder channel;

(6) Lobate Example 3 is interpreted to consist primarily of debrites including rafted blocks up to 200m in diameter. Minor turbidite, and hybrid event bed, deposits also may be present.

5. DISCUSSION OF MODEL VARIABILITY

When deep water lobate systems are interpreted from under-sampled data, as in subsurface reservoirs or discontinuous outcrops, it is appropriate to select a model, or variety of models, that are consistent with existing constraining data in order to guide characterization of the deposit. For example, an important factor influencing permeability architecture of lobate deposits is the presence of amalgamation and distributary channels (Pyles et al. 2014; Jones et al., 2015; Hofstra et al., 2016; Bell et al., 2018). Typically, the presence of distributary channels and other architectural features of fan lobes are inferred rather than observed directly and that inference is based on models.

Normark (1970, 1978), based on sparse, low resolution marine data, described a depositional lobe (herein referred to as the “Standard” Lobe Model) as being located at the terminus of a feeder channel within a submarine fan. The lobe itself displays further shallow distributary channels in the proximal lobe but few to none in the distal lobe. Recent submarine fan models (e.g. Prélat et al., 2009, 2010; Mulder and Etienne, 2010) still emphasize the linkage of depositional lobes to fan-scale feeder channels as well as the presence of distributary channels within the proximal portions of depositional lobes.

Although the “Standard” Lobe Model is widely used, we wish to emphasize that it is only one of several models and it should not be applied automatically to all lobate deposits. The “Standard” Lobe Model was proposed based on the best data available at the time. However, despite nearly 50 years of research since the model was proposed, we are unaware of any well constrained example of a lobate deposit that objectively confirms the “Standard” Lobe Model. Therefore it is critical to understand the range of potentially applicable models for lobate deposits.

Mulder and Etienne (2010) proposed that a distributary channel network in the proximal lobe develops if flows are mud-rich whereas poorly channelized lobes result from sand-dominated flows. Based on the examples described in this paper, for which we have no direct sampling of sediment caliber, we suggest that the mode of feeder channel confinement serves as a useful proxy for sediment caliber: i.e. a levee confined feeder channel implies mud-rich flows whereas erosionally-confined feeder channels without levees imply mud-poor flows. Consistent with this proposal, Lobate Example 1 displays an extensive system of distributary channels and a levee confined feeder channel. Lobate Example 2 does not display conventional distributary channels, only scours, at the mouth of one or more erosional feeder channels.

All three of the Lobate Examples of this study (summarized in Figure 9) differ from the “Standard” Lobe Model in some significant way based on the presence, absence, or distribution of distributary channels. Lobate Example 1 (Figures 1and 9) partially conforms to the “Standard” Lobe Model in that a levee-confined feeder channel leads to a system of avulsed levee-confined distributary channels. However, at the terminus of each levee-confined distributary channel, instead of unchannelized deposits, a pervasively channelized unit is present that is dominated by a cluster of sub-parallel to slightly divergent small channels. Thus the entirety of Lobate Example 1 (Figures 1 and 9) is covered by distributary channels with numerous avulsion nodes. The presence of well-developed levees confining the feeder and proximal distributary channels, as well as the acoustic variability required to yield well imaged channels, suggests that critical volumes of mud were transported and deposited within the system, at least in overbank settings, a conclusion that is compatible with the proposal of Mulder and Etienne (2010). However, even their model for channelized lobes does not illustrate the high density of distributary channels present in Lobate Example 1 (Figures 1 and 9).

In contrast, Lobate Example 2 (Figures 5 and 9) appears to have no distributary channels and a much higher aspect ratio (300:1) than Lobate Example 1 (108:1) (Table 1). The source of sediments deposited in Example 2 appears to be littoral drift at the contemporaneous shelf edge, which is likely to be overwhelmingly sand-rich (Imhansoloeva et al., 2011). Thus the absence of distributary channels is consistent with the proposal of Mulder and Etienne (2010). Other Lobate Examples without distributary channel systems have been imaged and described. Most notably, Lobe X of Prather et al. (2012a) and Jobe et al. (2017) is located approximately 100 km to the northwest of Lobate Example 2 and buried to a similar depth. Seismic data from Lobe X (60 Hz, 12.5m X 18.75m bin spacing) is very similar in resolution to the data set illustrated here (Figures 3-6). Multiple cores from Lobe X confirm that it is very sand-rich.

Lobate Example 3 (Figures 7 and 9) conforms superficially to the “Standard” Lobe Model but differs in that the few distributaries that avulse at the mouth of the feeder channel extend without further avulsions to the observed limits of the lobate deposit. Although, of the three examples, the gross architecture of Lobate Example 3 most closely resembles the “Standard” Lobe Model, it appears to be constructed predominantly by mass flow deposits rather than turbidites.

Thus, in addition to the “Standard” Lobe Model, updated in Prélat et al. (2009, 2010), there are at least 3 additional architectural models to consider and guide interpretation of unconfined deposits (Figure 10). Recognition of these separate models is significant in that their architecture is consistent with the suggestions of Mulder and Etienne (2010) that lobate deposits with a well-developed distributary channel system appear to be relatively mud-rich whereas sand-rich deposits have no distributaries. Further, the recognition of debrite-dominated lobate bodies predicts a high risk for the presence of clean and connected sands.

5.1 Subsurface and modern analogs

High resolution reflection seismic data of features at or near the seabed provide the most robust, three dimensional images of submarine lobate bodies. However, with few exceptions (Migeon et al., 2010; Jobe et al., 2017), core samples are sparse to non-existent. Imaging of submarine lobes often reveals few details of architectural features within the lobe or even on the lobe surface. These fine-scale features are best revealed by highest resolution bathymetric surveys but these surveys, with few exceptions (Maier et al., 2011; Carvajal et al., 2017; Maier et al., 2018), have rarely been conducted across submarine lobes.

In some cases, lens-shaped lobate deposits (Figure 8), typically stacked in a compensating pattern (sensu Mutti and Sonnino, 1981), can be recognized within a fan from reflection seismic data (e.g. Saller et al., 2008; Yang and Kim, 2014), but even these gross features may not be resolved unless near the seabed (e.g. Gervais et al., 2006; Deptuck et al., 2008; Bourget et al., 2010; Picot et al., 2016; Dannielou et al., 2017; Hamilton et al., 2017; and Jobe et al., 2017).

Within individual lobate deposits, unambiguous seismic images of distributary channel systems are uncommon in deeply buried deposits, though they may be imaged in some near surface examples (Kidd, 1999; Posamentier and Kolla, 2003; Hadler-Jacobsen et al., 2005, 2007; Clark and McHargue, 2007; Prather et al., 2012b; Bakke et al., 2013; Oluboyo et al., 2014). Curiously, in these examples, distributary channels tend to extend across the entire lobate body rather than just in the proximal portion. Incisional transient fan channels may be well imaged (Johann et al., 2001; Adeogba et al., 2005; Prather et al., 2012a; Barton, 2012; Yang and Kim, 2014). More common are lobate deposits with elongate to slightly divergent textures that might, ambiguously, be interpreted to represent distributaries (e.g. Jegou, et al., 2008; Shanmugam et al., 2009; Bourget et al., 2010; Migeon et al., 2010; Sylvester et al., 2012; Egawa et al., 2013).

If distributaries are not imaged, is that because they are difficult to image or because they are absent? It is understandable if distributaries are not well imaged. Lobate deposits typically represent sand-rich environments both within and surrounding distributary channels. Therefore, it may be common that the acoustic properties of the channel fill are similar to those of surrounding overbank deposits. With little impedance contrast, imaging of distributaries is poor. Yet, in Lobate Example 1 (Figure 1), distributaries are well imaged. Relatively mud-rich flows allowed for levee construction in proximal distributaries but also may have provided sufficient mud in overbank deposits of the middle to outer distributaries to provide impedance differentiation.

Distributaries may be present, even if not imaged, but it does not follow that one can assume their presence. Like Example 2, Jobe et al. (2014), based on detailed imaging, described a lobate deposit from Nigeria which has no distributaries. The absence of levees and distributaries in Example 2 (Figure 5) contrasts with the presence of both levees and distributaries in Example 1 (Figure 1). Are distributaries usually levee-confined (contrary to Normark 1978 and Mutti, 1979)? If so, are mud-rich flows necessary to develop a distributary system as suggested by Mulder and Etienne (2010)? This is an intriguing possibility. Perhaps some degree of bank stabilization, provided by the presence of clay, is necessary in order to construct distributaries, as in Lobate Example 1 (Figure 1). Sand-rich, mud-poor flows, as proposed for Lobate Example 2 (Figure 5), may collapse without the development of distributaries if reduced gradient is insufficient to sustain momentum. Flows with greater momentum scour and bypass without constructing distributaries.

So, if one cannot assume the presence of distributaries, how can one predict their presence or absence when none are imaged? To that end, we propose a hypothesis: in a lobate deposit, distributaries are likely if the feeder channel is levee confined (the clay content of the lobate deposits exceeds an as yet undefined threshold) whereas distributaries are unlikely if the feeder channel is erosionally confined (non-leveed).

Lobate deposits dominated by mass transport in Lobate Example 3 (Figure 7) are not unique. The example from Alfaro and Holz (2014) also appears to be dominated by debrites and shares most of the features displayed by Example 3. Debrite dominated lobate deposits also have been imaged with sidescan data and confirmed with core from the Mississippi (Twichell et al., 1992, 2009) and Nile (Ducassou et al., 2009; Migeon et al., 2010) submarine fans. However, given the very different tools with which these lobate bodies have been imaged versus Lobate Example 3, the architecture is hard to compare. Nevertheless, these examples suggest that debrite dominated lobate deposits may be common.

5.2 Outcrop analogs

It is challenging to reconcile architectural features illustrated in high resolution 3D reflection seismic data with observations from outcrops. Yet outcrop exposures are the principal way by which facies relationships within submarine lobate deposits are observed and documented. In order to relate outcrop-based facies observations to the architectural elements documented in reflection seismic data, it is critical to unambiguously recognize these elements in laterally continuous and extensively exposed outcrops. This has not always proven possible due to limitations of outcrop exposure, quality, and continuity. More often, models are used to guide the interpretation of outcrops rather than outcrops constraining models.

Multiple slightly diverging feeder channels have been reported from the Brushy Canyon Formation (Carr and Gardner, 2000; Gardner et al., 2003). In the Ross Formation of Ireland, feeder channels and incisional transient fan channels have been recognized and mapped, but not distributaries within lobes (Elliott, 2000; MacDonald et al., 2011; Pyles et al., 2014; Pierce et al., 2018). Likewise, in the Skoorsteenberg Formation of South Africa, probably the most extensively exposed lobate succession in the world, feeder channels are reported but distributaries are not recognized, at least not as conventional erosional channels (Hodgetts et al., 2004; Hodgson et al., 2006). Instead, what are seen repeatedly within lobate deposits of the Skoorsteenberg Formation are scours and zones of bed amalgamation (Johnson et al., 2001; Hodgetts et al., 2004; Hodgson et al., 2006; Prélat et al., 2010; Hofstra et al., 2015). Scours and zones of amalgamation also are common in other well exposed lobate deposits (e.g. Elliott, 2000; Carr and Gardner, 2000; Gardner et al., 2003; Remacha et al., 2005; MacDonald et al., 2011; Van der Merwe et al., 2014; Figueiredo et al., 2010). Scours, or megaflutes, are interpreted to be local features rather than through going distributary channels (Elliott, 2000; Hodgson et al., 2006; MacDonald et al., 2011; Hofstra et al., 2016), although scours and scour trains (cyclic steps) have been proposed as possible channel precursors (Fildani et al., 2006, 2013; Armitage et al., 2012; Maier et al., 2011, 2013; Covault et al., 2014, 2017).

Zones of bed amalgamation have been interpreted in the Skoorsteenberg Formation to represent the axes of distributive flows (depositional channels of Johnson et al., 2001). It is logical that zones of amalgamation represent locations of focused flow, and it is possible that these zones are present in a distributary pattern. Unfortunately, extensive work on these outcrops has not confirmed any particular pattern in map view (Hodgetts et al., 2004; Hodgson et al., 2006; Prélat et al., 2010). Also, it seems unlikely that the slight difference in the amount of mud within the preserved interbedded mud laminations of non-amalgamated areas versus zones of amalgamation would provide sufficient acoustic contrast to produce a channel image with distinct channel margins as displayed in reflection seismic images of Lobate Example 1 (Figure 1).

In rare contrast, erosional distributary channels have been reported from the Kaza Formation of the Windermere Group (Terlaky et al. 2016). It is possible that, because of vague definitions and inconsistencies in the use of terminology and hierarchy, lobe distributaries are more common than summarized here. For example, the multiple feeder channels of the Ongeluks River outcrop of the Skoorsteenberg Formation might be considered proximal distributaries although they are absent in the rest of the outcrop belt (Johnson et al., 2001; Hodgetts et al., 2004; Hodgson et al., 2006).

Despite these challenges in determining the presence, absence, and distribution of distributaries in outcrop exposures, published illustrations of proposed models of unconfined units in outcrop routinely resemble the “Standard” Lobe Model with a few distributaries in the proximal lobe and none in the middle and distal lobe (e.g. Hirayama and Nakajima, 1977; Eschard et al., 2004; Hodgson et al., 2009; Prélat et al., 2010; Bernhardt et al., 2011; MacDonald et al., 2011; Brunt et al., 2013; Etienne et al., 2013; So et al., 2013; Grundvag et al.,2014; Van der Merwe et al., 2014; Spychala et al., 2015; Masalimova et al., 2016; Terlaky et al., 2016; Kane et al., 2017). However, highest resolution bathymetric data have not confirmed the “Standard” Lobe Model (i.e. Carvajal et al., 2017). Furthermore, high resolution 3D seismic images, such as illustrated here (Figs. 1, 5, 7), indicate that unconfined lobate deposits are more diverse than any single model (Figure 10).

Outcrop analogs for the three lobate deposits described here are not obvious. The Kaza Formation (Terlaky et al. 2016) is most similar to Lobate Example 1(Figures 1 and 9) in that multiple scales of channels are present. However, channel density in the Kaza Formation apparently is inadequate to match that of Lobate Example 1. In fact the channels are so numerous in Lobe Example 1 that, in outcrop, it might not be recognized as a lobate deposit. Likewise, it is questionable if an outcrop dominated by mass transport deposits, such as Lobate Example 3 (Figures 7 and 9), would be recognized as a fan-related lobate deposit. The

Skoorsteenberg Formation records multiple feeder channels, or possibly proximal distributary channels, at the Ongeluks River outcrop but appears to lack channels within the rest of the deposits. The lack of distinct channels can be compared to Lobate Example 2 (Figures 5 and 9), but there are few distinct features in Lobate Example 2 to provide constraints. The Skoorsteenberg Formation fans (Lobe Complexes of Prélat et al., 2009) are larger than Example 2 and have been interpreted to display a strongly hierarchical structure, which is unlikely for Lobate Example 2. Possibly, prolonged deposition of multiple stacked and/or offset lobate deposits like Example 2 could resemble Skoorsteenberg Fan 3, but this is speculative.

5.3 Processes

We have explained the morphology of lobate deposits and their associated channels as products of specific processes and mud concentration (Figures 9 and 10). Turbulent density stratified mud-rich flows produce levee-confined feeder channels and proximal distributaries, and multiple secondary and tertiary distributaries with many avulsion nodes (Lobate Example 1, Figures 1 and 2). Mud-poor turbidity currents, likely sourced from littoral drift or effective filtering of mud through flow stripping in long slope conduits, are prone to collapse and result in a lobate deposit with scour features but no distributaries (Lobate Example 2, Figures 3 through 6). Debris (laminar) flow dominated lobate features display straight, erosional feeder channels, a small number of straight distributary channels emanating from the mouth of the feeder channel, and minimal avulsion nodes (Lobate Example 3, Figures 7 and 8).

Flows in Lobate Example 1 may be thin enough, after passing through a succession of avulsions, to allow the development of braided or multi-thread channels (Foreman et al., 2015). Because multi-thread channels are rarely reported in submarine settings, it is unclear what they might look like in high resolution reflection seismic data, but perhaps the distal channel clusters of Lobate Example 1 are candidates.

In Lobate Example 2, the absence of distributaries or levees is attributed to flow collapse with some scouring. If one accepts the interpretation that Lobate Example 2 is composed of sediments derived from littoral drift, then delivered sediment is very sand-rich with minimal mud, consistent with the absence of levees. Cohesion is minimal so these sediments are easily scoured (e.g. Hir et al., 2008). Although initial erosion of the substrate may be a prerequisite for channel initiation (Fildani et al., 2013), parallel sided channels did not form in Lobate Example 2; consistent with the conclusion of Rowland et al. (2010) that cohesive banks are necessary to produce parallel sided channels in flume experiments. However, elongate scours with distally divergent margins, as seen in Lobate Example 2, are similar to features generated in non-cohesive sediments in flumes (e.g. Metivier et al., 2005, their Figure 2; and Cantelli et al., 2011, their Figures 1 and 4) and in at least one example of very high resolution bathymetry from a channel-lobe transition (Carvajal et al., 2017).

In Lobate Example 3, the straight erosional feeder channel and sparse straight distributaries without secondary evulsions resemble features deposited from laminar flows in a flume (Fernandez et al., 2014). The morphology of Lobate Example 3 also is similar to debris flow deposition on subaerial fans (Figure 11A) with long straight distributaries and few avulsions. This morphology contrasts sharply with the pervasive distributaries and abundant avulsion nodes of subaerial fans dominated by turbulent flows (Figure 11B) which have more features in common with the distributary architecture of Lobate Example 1. The two subaerial fans also differ in grain size populations aligned with their submarine counterparts. The debris flow dominated subaerial fan (Figure 11A) contains more mud (primarily as matrix) than the fan dominated by turbulence which consists mostly of gravel and sand (Figure 11B).

The significance of differences in aspect ratios in unconfined lobate deposits is unclear but may provide evidence of the dominant responsible process. For the three examples studied here (Table 1), collapse of sand-rich flows, Lobate Example 2, produces a thin deposit (W/T = 300/1). Relatively mud-rich turbulent flows, Lobate Example 1, produce a much thicker deposit relative to width (W/T = 108). The debris flow dominated deposit, Lobate Example 3, displays intermediate dimensions and an intermediate aspect ratio (W/T = 163). All three of these examples fall within the “confined” cluster of Prélat et al., (2010). We should point out that two of our examples (Lobate Examples 1 and 3) are also included in the six deposits they measured (their Nigeria and Indonesia examples respectively).

Although the settings are radically different, it is interesting that turbulent flows in both subaerial and submarine settings are capable of generating similar distributive architectures. Likewise, laminar flows in both settings are capable of producing distributive architectures that, though similar to Lobate Example 3, are distinctly different from the architectures formed from turbulent flows. These two examples suggest that further, more detailed and quantitative comparisons to subaerial fans might prove useful for developing predictive models of submarine lobate deposits.

5.4 Classification

Application of the “Standard” Lobe Model is problematic. The model (Normark, 1970, 1978 and Mutti and Ghibaudo, 1972) loosely defined a lobe as part of a submarine fan consisting of a lobate sand-rich deposit at the distal end of a feeder channel and containing a distributary channel system in its proximal part. However, lobate depositional bodies can be present at multiple scales with a variety of architectures and permeability structures. If we restrict the term lobe to the original definition, then what should non-conforming lobate bodies be called? Instead, it seems advisable to accept a broader definition of the term lobe and differentiate diverse architectures with a standardized set of descriptors such as "pervasively channelized lobe" or "unchannelized lobe". This approach is flexible and can be adapted as new architectures are recognized. Unfortunately, the term "lobe" has been used to label one level within a hierarchy of lobate architectures (Prélat, et al., 2009; Groenenberg et al., 2010; Mulder and Etienne, 2010; and Prélat and Hodgson, 2013) with an informal and empirical range of external dimensions (Prélat, et al., 2009). We suggest that it is confusing and undesirable to use a common morphological term such as lobe to also designate one particular scale within a hierarchy of lobate bodies.

5.5 Hierarchy

The outcrop belt of lobate deposits that is most intensely studied and extensively exposed is the Skoorsteenberg Formation in the Tanqua Karoo Basin, South Africa (e.g. Johnson et al., 2001; Hodgson et al., 2006; Prélat, et al., 2009; Groenenberg et al., 2010; and Prélat and Hodgson, 2013). These deposits have been interpreted to display a hierarchy of tabular, lobate sandstone bodies that systematically increase in thickness and lateral extent with increasing rank. Furthermore, each higher rank within the sandstone hierarchy is separated by a siltstone unit that correspondingly also increases in thickness (Prélat et al., 2009). This scheme has been adopted by other researchers for other lobate deposits (e.g. Mulder and Etienne, 2010). Straub and Pyles (2012) discussed the difference between hierarchical structure and self-similar structure in lobate deposits and provided cartoons to illustrate the difference (their Figure 1). Although correlation cross-sections of the Skoorsteenberg deposits (Prélat et al, 2009, their Figure 13) compare well with hierarchical structure as illustrated by Straub and Pyles (2012, their Figure 1A), the summary cartoon of Prélat et al. (2010, their Figure 2) could be interpreted to represent a fractal structure as illustrated by Straub and Pyles (2012, their Figure 1B). This ambiguity reflects the difficulty of constraining 3-dimensional structure from limited outcrop data, even in the best of circumstances.

In theory, each unit within a hierarchical level is separated from the others by avulsion. A plan view map of units is most helpful for recognizing avulsions imaged by reflection seismic data although ambiguity remains. Furthermore, terminology is a recurring issue. A feeder channel at a fine scale may accurately be called part of a distributary channel system at a larger scale. In Lobate Example 1 for example (Figure 1), so many avulsions are imaged at so many scales that it is difficult to keep track of how many levels within a hierarchy would be required. Or, more likely, Lobate Example 1 has a fractal structure (Straub and Pyles, 2012). On the other extreme, the absence of channel avulsions in Lobate Example 2 (Figure 5) provides no basis for a hierarchical structure linked to avulsions. Lobate Example 3 (Figure 7), because of the presence of a few distributary channels and at least one avulsion node, suggests the possible presence of a hierarchical structure.

However, without bed scale lithologic data, the assignment of specific hierarchical terms as defined by Prélat et al. (2009) for the Skoorsteenberg Formation is ambiguous based on reflection seismic data alone. The three examples described here are much too thick relative to their lateral extent to equate with any of the hierarchical units defined by Prélat et al. (2009). Possibly the lobate bodies imaged in reflection seismic data extend laterally beyond the imaged limits because of inadequate resolution. If so, based on their thickness, these lobate deposits might equate with Lobe Complexes of Prélat et al. (2009). Alternatively, the Skoorsteenberg hierarchy might not be transferrable to the lobate units described here.

6. CONCLUSIONS

1. The "Standard" Lobe Model, an unconfined lobate deposit with proximal distributary channels and unchannelized medial to distal deposits fed through a single levee-confined feeder channel, is widely applied to guide interpretation of unconfined deep marine deposits. However, this model has not been confirmed by any high resolution data set and its validity is questionable. Alternative models of unconfined architectures are sorely needed.
2. Three models presented here illustrate some of the diversity of architectures to be found in unconfined deposits and provide alternative models to guide interpretation (Figures 9 and 10).
    a. Lobate Example 1 (Figures 1 and 2), a feature with prominent distributary channels, is interpreted to display the following characteristics: (1) sediments are transported to the lobate deposit via a single levee-confined channel complex, (2) delivered sediments are heterolithic, including enough mud in the upper dilute portion of flows to allow for levee construction, (3) sediments are dispersed across the lobate deposit via an extensive system of distributary channels, (4) the proximal distributary channels were levee confined, (5) the lobate deposit grows as a result of avulsions or bifurcations at numerous and diverse nodes along the distributary channel pathways, and (6) the resulting deposit is pervasively channelized to the imaged limits of the lobate deposit.

b. Lobate Example 2 (Figures 3 through 6), a lobate feature without distributary channels, is interpreted to display the following characteristics: (1) it is constructed of sediments derived from multiple points along the shelf edge (a line source) without evidence of a submarine canyon, (2) the line source reflects remobilized littoral drift intercepted and remobilized at slump scars at or near the shelf edge, (3) the delivered sediments are transported from the shelf edge to the lobate deposit via multiple erosional gullies or erosional channel complexes that are focused by slope topography toward the location of the lobate deposit, (4) feeder channels and lobate deposits lack any resolvable levees suggesting that the delivered sediments are extremely sand-rich with minimal accompanying mud, (5) no distributary channel system is visible within the lobate deposit although elongate scours are interpreted, and (6) deposition is interpreted to result from flow collapse although occasional robust flows scour and bypass previous deposits.

c. Lobate Example 3 (Figures 7 and 8), a feature with few long, straight distributaries, is interpreted to display the following characteristics: (1) it is located at the end of a straight, erosional feeder channel without discernable levees, (2) it displays a “nodular” seismic character in plan view, typical of mass transport deposits, with individual nodules representing rafted blocks up to 200m wide, (3) a small number (<5) of long, straight distributary channels avulse at the mouth of the feeder channel, (4) distributaries extend without further avulsion to near the end of the lobate deposit, and (5) the long, straight, non-avulsing channels are interpreted to result primarily from laminar flows (debris flows) although minor turbidite and hybrid event deposits also may be present.

3. We have explained the morphology of lobate deposits and their associated channels as products of specific processes and mud concentration. Mud-rich turbidity currents produce levee-confined feeder channels, levee-confined proximal distributaries, and multiple secondary and tertiary distributaries with many avulsion nodes (Lobate Example 1, Figure 10A). Mud-poor turbulent flows, likely sourced from littoral drift, are prone to collapse and result in a lobate deposit with scour features but no distributaries (Lobate Example 2, Figure 10B). Debris (laminar) flow dominated lobate features display straight, erosional feeder channels, a small number of straight distributary channels emanating from the mouth of the feeder channel, and minimal avulsion nodes (Lobate Example 3, Figure 10C).
4. Outcrop analogs for the three lobate deposits described here are not obvious. For example, it is likely that a pervasively channelized outcrop, as would be produced by a lobate deposit like Lobate Example 1, might not be interpreted as a lobate deposit.
5. It is unclear how zones of amalgamation, which are common in outcrops of lobate deposits outcrops, will appear in horizon-referenced displays from 3D reflection seismic data. However, we think it unlikely that they could look like conventional channels or distributaries.
6. With regard to terminology, we recommend a broad definition of the term lobe. Diverse architectures can be differentiated by using a standardized set of

descriptive qualifiers such as “pervasively channelized lobe” or “unchannelized lobe”. This approach is flexible and can be adapted as new architectures are recognized.

7. Without bed scale lithologic data, the assignment of specific hierarchical terms as defined by Prélat et al. (2009) for the Skoorsteenberg Formation is ambiguous based on reflection seismic data alone. For example, Lobate Example 1 may have a fractal structure and Lobate Example 2, without distributaries, lacks a basis for defining a hierarchy. Lobate Example 3 could have a hierarchical structure but it is much thicker than any of the hierarchical units of Prélat et al. (2009).
8. It is prudent to incorporate a high degree of uncertainty in models of sand-rich lobate deposits in the subsurface. Lobate deposits are diverse with a significant range of permeability architectures. The percentage of lobate deposits with distributary systems versus lobate deposits without distributary systems is unknown and the architecture and mode of confinement in distributary channels, if present, may vary across lobate deposits as well as across submarine fans.
9. Detailed quantitative comparisons to subaerial fans are useful for developing models of submarine lobate deposits.

7. ACKNOWLEDGEMENTS

The authors would like to thank Chevron Nigeria Ltd. and the Nigerian National Petroleum Co. for permission to publish the data for this research. Also we thank Chevron Indonesia and Pertamina for permission to publish data. The research was supported through the Stanford Project on Deep-Water Depositional Systems by AERA, Anadarko, Aramco Services

Company, California Resources Corporation, Chevron, Conoco-Phillips, Hess, Nexen, Pemex, PTTEP, RAG, Schlumberger, Shell, Woodside, and YPF.

8. REFERENCES CITED

Adeogba, A.A., McHargue, T.R., Graham, S.A., 2005. Transient fan architecture and depositional controls from near-surface 3-D seismic data, Niger Delta continental slope: American Association of Petroleum Geologists Bulletin 89, 627–643.

Alfaro, E. Holz, M., 2014. Seismic geomorphological analysis of deepwater gravity-driven deposits on a slope system of the southern Colombian Caribbean margin. Marine and Petroleum Geology 57, 294-311.

Allen, J.R.L., 1965. Late Quaternary Niger Delta, and adjacent areas - sedimentary environments and lithofacies: American Association of Petroleum Geologists Bulletin 49, 547–800.

Armitage, D.A., McHargue, T., Fildani, A., Graham, S.A., 2012. Postavulsion channel evolution: Niger Delta continental slope. American Association of Petroleum Geologists Bulletin 96, 823–843.

Bakke, K., Kane, I.A., Martinsen, O.J., Petersen, S.A., Johansen, T.A., Hustoft, S., Jacobsen, F.H.,Groth, A., 2013. Seismic modeling in the analysis of deep-water sandstone termination styles. Geohorizon. American Association of Petroleum Geologists Bulletin 97, 1395-1419.

Barton, M.D., 2012. Evolution of an intra-slope apron, offshore Niger Delta slope: Impact of step geometry on apron architecture. In: Prather, B.E., Deptuck, M.E., Mohrig, D., Van Hoorn, B., and Wynn, R.B. (Eds.), Application of the principles of seismic geomorphology to continental slope and base-of-slope systems: case studies from seafloor and near-seafloor analogues. SEPM Special Publication 99, 181–197.

Beaubouef, R.T., Rossen, C., Zelt, F.B., Sullivan, M.D., Mohrig, D.C., Jennette, D.C., 1999. Deep-Water Sandstones, Brushy Canyon Formation, West Texas. AAPG Hedberg Field Research Conference, American Association of Petroleum Geologists, Tulsa, Oklahoma, USA.

Bell, D., Kane, I.A., Pontén, A.S., Flint, S.S., Hodgson, D.M. and Barrett, B.J., 2018. Spatial variability in depositional reservoir quality of deep-water channel-fill and lobe deposits. Marine and Petroleum Geology 98, 97-115.

Bernhardt, A., Jobe, Z.R., Lowe, D.R., 2011. Stratigraphic evolution of a submarine channel–lobe complex system in a narrow fairway within the Magallanes foreland basin, Cerro Toro Formation, southern Chile. Marine and Petroleum Geology 28, 785-806.

Biscara, L., Mulder, T., Hanquiez, V., Marieu, V., Crespin, J.P., Braccini, E., Garlan, T., 2013. Morphological evolution of Cap Lopez Canyon (Gabon): illustration of lateral migration processes of a submarine canyon. Marine Geology 340, 49-56.

Bonnel, C., Dennielou, B., Droz, L., Mulder, T., Berne, S., 2005. Architecture and depositional pattern of the Rhône neofan and recent gravity activity in the Gulf of Lions (Western Mediterranean). Marine and Petroleum Geology 22, 827–843, doi:10.1016/j.marpetgeo.2005.03.003.

Bourget, J., Zaragosi, S., Mulder, T., Schneider, J.-L., Garlan, T., Van Toer, A., Mas, V., Ellouz-Zimmermann, N., 2010. Hyperpycnal-fed turbidite lobe architecture and recent sedimentary processes: A case study from the Al Batha turbidite system, Oman margin. Sedimentary Geology 229, 144–159.

Brunt, R.L., Di Celma, C.N., Hodgson, D.M., Flint, S.S., Kavanagh, J.P., van der Merwe, W.C., 2013. Driving a channel through a levee when the levee is high: An outcrop example of submarine down-dip entrenchment. Marine and Petroleum Geology 41, 134-145.

Burke, K., 1972. Longshore drift, submarine canyons, and submarine fans in development of Niger Delta. American Association of Petroleum Geologists Bulletin 56, 1975-1983.

Campion, K.M., Sprague, A.R., Mohrig, D., Lovell, R.W., Drzewiecki, P.A., Sullivan, M.D., Ardill, J.A., Jensen, G.N., Sickafoose, D.K., 2000. Outcrop expression of confined channel complexes. In: Weimer, P., Slatt, R.M., Bouma, A.H., and Lawrence, D.T. (Eds.), Deep-water reservoir of the world. Gulf Coast Section SEPM Foundation 20th Annual Research Conference, 127-150.

Cantelli, A., Pirmez, C., Johnson, S., Parker, G., 2011. Morphodynamic and stratigraphic evolution of self-channelized subaqueous fans emplaced by turbidity currents. Journal of Sedimentary Research. 81, 233–247. doi: 10.2110/jsr.2011.20

Carr, M., and Gardner, M.H., 2000, Portrait of a basinfloor fan for sandy deepwater systems, Permian Lower Brushy Canyon Formation, West Texas. In: Bouma, A. H., and Stone, C. G. (Eds.), Fine-grained turbidite systems. American Association of Petroleum Geologists Memoir 72/SEPM Special Publication 68, 215–232.

Carvajal, C., Paull, C.K., Caress, D.W., Fildani, A., Lundsten, E., Anderson, K., Maier, K.L., McGann, M., Gwiazda, R., Herguera, J.C., 2017. Unraveling the Channel–Lobe Transition

Zone With High-Resolution AUV Bathymetry: Navy Fan, Offshore Baja California, Mexico. Journal of Sedimentary Research 87, 1049-1059.

Clark, J., and McHargue, T., 2007. Stratigraphic and Spatial Changes in Channel Morphology Related to Deepwater Processes in Confined and Ponded Slope Mini-Basins, Angola. American Association of Petroleum Geologists, AAPG Search and Discover Article #90063 AAPG Annual Convention, Long Beach, California.

Covault, J.A., Kostic, S., Paull, C.K., Ryan, H.F., Fildani, A., 2014. Submarine channel initiation, filling and maintenance from sea-floor geomorphology and morphodynamic modelling of cyclic steps. Sedimentology 61, 1031–1054.

Covault, J.A., Kostic, S., Paull, C.K., Sylvester, Z., Fildani, A., 2017. Cyclic steps and related supercritical bedforms: building blocks of deep-water depositional systems, western North America. Marine Geology 393, 4-20.

Damuth, J.E., 1994. Neogene gravity tectonics and depositional processes on the deep Niger Delta continental margin. Marine and Petroleum Geology 11, 320–346.

Dennielou, B., Jallet, L., Sultan, N., Jouet, G., Giresse, P., Voisset, M., Berné, S., 2009. Post-glacial persistence of turbiditic activity within the Rhône deep-sea turbidite system (Gulf of Lions, Western Mediterranean): Linking the outer shelf and the basin sedimentary records. Marine Geology 257, 65–86.

Dennielou, B., Droz, L., Babonneau, N., Jacq, C., Bonnel, C., Picot, M., Le Saout, M., Saout, Y., Bez, M., Savoye, B., Olu, K., 2017. Morphology, structure, composition and build-up processes of the active channel-mouth lobe complex of the Congo deep-sea fan with inputs from remotely operated underwater vehicle (ROV) multibeam and video surveys. Deep Sea Research Part II. Topical Studies in Oceanography 142, 25-49.

Deptuck, M. E., Piper, D.J.W., Savoye, B., Gervai,s A., 2008. Dimensions and architecture of late Pleistocene submarine lobes off the northern margin of East Corsica. Sedimentology 55, 869 – 898.

Doughty-Jones, G., Mayall, M., Lonergan, L., 2017. Stratigraphy, facies, and evolution of deep-water lobe complexes within a salt-controlled intraslope minibasin. American Association of Petroleum Geologists Bulletin 101, 1879-1904.

Doust, H., and Omatsola, E., 1990, Niger Delta. In: Edwards, J. D., and Santagrossi, P. A. (Eds.), Divergent/Passive Margin Basins. American Association of Petroleum Geologists Memoir 45, 201– 238.

Ducassou, E., Migeon, S., Mulder, T., Murat, A., Capotondi, L., Bernasconi, S.M., Mascle, J., 2009. Evolution of the Nile deep-sea turbidite system during the Late Quaternary: influence of climate change on fan sedimentation. Sedimentology 56, 2061-2090.

Egawa, K., Furukawa, T., Saeki, T., Suzuki, K.,Narita, H., 2013. Three-dimensional paleomorphologic reconstruction and turbidite distribution prediction revealing a Pleistocene confined basin system in the northeast Nankai Trough area. American Association of Petroleum Geologists Bulletin. 97, 781-798.

Elliott, T., 2000. Depositional architecture of a sand-rich, channelised turbidite system: the Upper Carboniferous Ross Sandstone Formation, Western Ireland. In: Weimer, P., Slatt, R.M., Coleman, J., Rossen, N.C., Nelson, H., Bouma, A.H., Styzen, M.J. (Eds.), Deep-Water

Reservoirs of the World. Gulf Coast Section SEPM Foundation 20th Annual Research Conference, 342–364.

Eschard, R., Albouy, E., Gaumet, F.,Ayub, A., 2004. Comparing the depositional architecture of basin floor fans and slope fans in the Pab Sandstone, Maastrichtian, Pakistan. Geological Society, London, Special Publications 222, 159-185.

Etienne, S., Mulder, T., Razin, P., Bez, M., Désaubliaux, G., Joussiaume, R.,Tournadour, E., 2013. Proximal to distal turbiditic sheet-sand heterogeneities: Characteristics of associated internal channels. Examples from the Trois Evêchés area, Eocene-Oligocene Annot Sandstones (Grès d'Annot), SE France. Marine and Petroleum Geology 41, 117-133.

Fernandez, R.L., Cantelli, A., Pirmez, C., Sequeiros, O.,Parker, G., 2014. Growth Patterns of Subaqueous Depositional Channel Lobe Systems Developed Over A Basement With A Downdip Break In Slope: Laboratory Experiments. Journal of Sedimentary Research 84, 168-182.

Figueiredo, J.J., Hodgson, D.M., Flint, S.S.,Kavanagh, J.P., 2010. Depositional environments and sequence stratigraphy of an exhumed Permian mudstone-dominated submarine slope succession, Karoo Basin, South Africa. Journal of Sedimentary Research 80, 97-118.

Fildani, A., Normark, W.R., Kostic, S., Parker, G., 2006. Channel formation by flow stripping: large-scale scour features along the Monterey East Channel and their relation to sediment waves. Sedimentology 53, 1265–1287.

Fildani, A., Hubbard, S.M., Covault, J.A., Maier, K.L., Romans, B.W., Traer, M., Rowland, J.C., 2013. Erosion at inception of deep-sea channels. Marine and Petroleum Geology 41, 48-61. doi:10.1016/j.marpetgeo.2012.03.006.

Foreman, B.Z., Lai, S.Y., Komatsu, Y.,Paola, C., 2015. Braiding of submarine channels controlled by aspect ratio similar to rivers. Nature Geoscience 8, 700-703.

Fowler, J.N., Guritno, E., Sherwood, P.,Smith, M.J., 2001. IPA01-G-120. Depositional Architectures of Recent Deep Water Deposits in the Kutei Basin, East Kalimantan. In Proceedings of the Annual Convention-Indonesian Petroleum Association 1, 409-422. Indonesian Petroleum Association; 1998.

Gamberi, F., Rovere, M., 2011. Architecture of a modern transient slope fan (Villafranca fan, Gioia basin–Southeastern Tyrrhenian Sea). Sedimentary Geology 236, 211–225.

Gardner, M.H., Borer, J.M., Melick, J.J., Mavilla, N., Dechesne, M., Wagerle, R.N., 2003. Stratigraphic process-response model for submarine channels and related features from studies of Permian Brushy Canyon outcrops, West Texas. Marine and Petroleum Geology 20, 757–787, doi:10.1016/j.marpetgeo.2003.07.004.

Gervais, A., Savoye, B., Mulder, T., Gonthier, E., 2006. Sandy modern turbidite lobes: A new insight from high resolution seismic data. Marine and Petroleum Geology 23, 485–502.

Gorsline, D. S., Emery, K. O., 1959. Turbidity-current deposits in San Pedro and Santa Monica basins off southern California. Geological Society of America Bulletin 70, 279–290.

Groenenberg, R.M., Hodgson, D.M., Prélat, A., Luthi, S.M., Flint, S.S., 2010. Flow–deposit interaction in submarine lobes: Insights from outcrop observations and realizations of a process-based numerical model. Journal of Sedimentary Research 80, 252–267, doi: 10.2110/jsr.2010.028.

Grundvåg, S.A., Johannessen, E.P., Helland-Hansen, W.,Plink-Björklund, P., 2014. Depositional architecture and evolution of progradationally stacked lobe complexes in the Eocene Central Basin of Spitsbergen. Sedimentology 61, 535-569.

Hadler-Jacobsen, F., Johannessen, E.P., Ashton, N., Henriksen, S., Johnson, S.D.,Kristensen, J.B., 2005. January. Submarine fan morphology and lithology distribution: a predictable function of sediment delivery, gross shelf-to-basin relief, slope gradient and basin topography. Geological Society, London, Petroleum Geology Conference series 6, No. 1, 1121-1145). Geological Society of London.

Hadler-Jacobsen, F., Gardner, M. H., Borer, J. M., 2007. Seismic stratigraphic and geomorphic analysis of deep-marine deposition along the West African continental margin. In: Davies, R.J., Posamentier, H.W., Wood, L.J., and Cartwright, J.A. (Eds.), seismic geomorphology: applications to hydrocarbon exploration and production: London, Geological Society [London] Special Publication 277, 47-84, doi: 10.1144/GSL.SP.2007.277.01.04.

Hamilton, P., Gaillot, G., Strom, K., Fedele, J., Hoyal, D., 2017. Linking Hydraulic Properties In Supercritical Submarine Distributary Channels To Depositional-Lobe Geometry. Journal of Sedimentary Research 87, 935-950.

Hanquiez, V., Mulder, T., Toucanne, S., Lecroart, P., Bonnel, C., Marchès, E., Gonthier, E., 2010. The sandy channel–lobe depositional systems in the Gulf of Cadiz: Gravity processes forced by contour current processes. Sedimentary Geology 229, 110–123.

Hir, P.L., Cann, P., Waeles, B., Jestin, H., Bassoullet, P., 2008. Chapter 11: Erodibility of natural sediments: experiments on sand/mud mixtures from laboratory and field erosion tests. In: Kusuda, T., Hiroyuki, Y., Spearman, J., Gailani, J.Z. (Eds.), Proceedings in Marine Science 9: Amsterdam, Elsevier, 137–153.

Hirayama, J.,Nakajima, T., 1977. Analytical study of turbidites, Otadai Formation, Boso Peninsula, Japan. Sedimentology 24, 747-779.

Hodgetts, D., Drinkwater, N.J., Hodgson, D.M., Kavanagh, J.P., Flint, S.S., Keogh, K.J., Howell, J.A., 2004. Three-dimensional geological models from outcrop data using digital data collection techniques: an example from the Tanqua Karoo depocentre, South Africa. In: Curtis, A.C., and Wood, R. (Eds.), Geological prior information: informing science and engineering. London, Geological Society [London] Special Publication 239, 57–75.

Hodgson, D.M., Flint, S.S., Hodgetts, D., Drinkwater, N.J., Johannessen, E.P., Luthi, S.M., 2006. Stratigraphic evolution of fine-grained submarine fan systems, Tanqua depocenter, Karoo Basin, South Africa. Journal of Sedimentary Research 76, 20–40, doi: 10.2110/jsr.2006.03.

Hodgson, D.M., 2009. Distribution and origin of hybrid beds in sand-rich submarine fans of the Tanqua depocentre, Karoo Basin, South Africa. Marine and Petroleum Geology 26, 1940-1956.

Hofstra, M., Hodgson, D.M., Peakall, J.,Flint, S.S., 2015. Giant scour-fills in ancient channel-lobe transition zones: Formative processes and depositional architecture. Sedimentary Geology 329, 98-114.

Hofstra, M., Pontén, A.S.M., Peakall, J., Flint, S.S., Nair, K.N.,Hodgson, D.M., 2016. The impact of fine-scale reservoir geometries on streamline flow patterns in submarine lobe deposits using outcrop analogues from the Karoo Basin. Petroleum Geoscience 23, 2016-087.

Imhansoloeva, T.M., Akintoye, A.E., Mayowa, I.P., Abdulkarim, R., Oguwuike, I.D., Olubukola, S.,Ruth, F.B., 2011. Numerical assessment and analysis of textural deposits of beach sediment: A case study of Ajah (Okun Mopo) Beach Lagos South West Nigeria. Nature and Science 9, 165-174.

Jegou, I., Savoye, B., Pirmez, C., Droz, L., 2008. Channel-mouth lobe complex of the recent Amazon Fan: the missing piece. Marine Geology 252, 62-77.

Jobe, Z. R., Z. Sylvester, C. Pirmez, B. Prather, S. A. El-Gawad, D. Minisini, A. Cantelli, N. Howes, R. Smith, 2014. Ultra-high resolution modern analog dataset from the Western Niger Delta Slope: Facies architecture and application to turbidite reservoirs. Gulf Coast Association of Geological Societies Transactions 64, 543–546.

Jobe, Z.R., Sylvester, Z., Parker, A.O., Howes, N., Slowey, N., Pirmez, C., 2015. Rapid Adjustment of Submarine Channel Architecture to Changes in Sediment Supply. Journal of Sedimentary Research 85, 729-753.

Jobe, Z.R., Sylvester, Z., Howes, N., Pirmez, C., Parker, A., Cantelli, A., Smith, R., Wolinsky, M.A., O’Byrne, C., Slowey, N., Prather, B., 2017. High-resolution, millennial-scale patterns of bed compensation on a sand-rich intraslope submarine fan, western Niger Delta slope. Geological Society of America Bulletin 129, 23-37.

Johann, P., de Castro, D.D., Barroso, A.S., 2001, January. Reservoir geophysics: Seismic pattern recognition applied to ultra-deepwater oilfield in Campos basin, offshore Brazil. In: SPE Latin American and Caribbean Petroleum Engineering Conference. Society of Petroleum Engineers SPE 69483.

Johnson, S.D., Flint, S., Hinds, D., De Ville Wickens, H., 2001. Anatomy, geometry and sequence stratigraphy of basin floor to slope turbidite systems, Tanqua Karoo, South Africa. Sedimentology 48, 987-1023.

Jones, D.W., Large, S., McQueen, A., Helmi, A., 2015. Reservoir geology of the Paleocene Forties Sandstone Member in the Fram discovery, UK Central North Sea. Geological Society, London, Special Publications 403, SP403-13, 219-246.

Kane, I.A., Pontén, A.S., Vangdal, B., Eggenhuisen, J.T., Hodgson, D.M., Spychala, Y.T., 2017. The stratigraphic record and processes of turbidity current transformation across deep-marine lobes. Sedimentology 64, 1236-1273.

Ketzer, J.M., Carpentier, B., Le Gallo, Y., Le Thiez, P., 2005. Geological sequestration of CO2 in mature hydrocarbon fields. Basin and reservoir numerical modelling of the Forties Field, North Sea. Oil & gas science and technology 60, 259-273.

Kidd, G.D., 1999. Fundamentals of 3-D seismic volume visualization. The Leading Edge 18, 702-709.

Lowry, P., Jenkins, C.D., Phelps, D.J., 1993, January. Reservoir scale sandbody architecture of Pliocene turbidite sequences, Long Beach Unit, Wilmington oil field, California. In: SPE Annual Technical Conference and Exhibition. Society of Petroleum Engineers. SPE 26440.

MacDonald, H.A., Peakall, J., Wignall, P.B., Best, J., 2011. Sedimentation in deep-sea lobe-elements: implications for the origin of thickening-upward sequences. Journal of the Geological Society [London] 168, 319–331, doi: 10.1144/0016-76492010-036.

Maier, K.L., Fildani, A., Paull, C.K., Graham, S.A., McHargue, T., Caress, D., McGann, M., 2011. The elusive character of discontinuous deep-water channels: new insights from Lucia Chica channel system, offshore California. Geology 39, 327-330.

Maier, K.L., Fildani, A., McHargue, T., Paull, C.K., Graham, S.A., Caress, D.W., 2012. Deep-water punctuated channel migration: high-resolution subsurface data from the Lucia Channel System, offshore California. Journal of Sedimentary Research 82, 1-8.

Maier, K.L., Fildani, A., Paull, C.K., McHargue, T.R., Graham, S.A., Caress, D.W., 2013. Deep-sea channel evolution and stratigraphic architecture from inception to abandonment from high-resolution Autonomous Underwater Vehicle surveys offshore central California. Sedimentology 60, 935–960.

Maier, K.L., Roland, E.C., Walton, M.A., Conrad, J.E., Brothers, D.S., Dartnell, P. and Kluesner, J.W., 2018. The Tectonically Controlled San Gabriel Channel–Lobe Transition Zone, Catalina Basin, Southern California Borderland. Journal of Sedimentary Research 88, 942-959.

Martinsen, O.J., Lien, T., Walker, R.G., Lien, T., 2000. Upper Carboniferous deep water sediments, western Ireland: Analogues for passive margin turbidite plays. In: Weimer, P., Slatt, R.M., Coleman, J., Rosen, N.C., Nelson, H., Bouma, A.H., Styzen, M.J., Lawrence, D.T. (Eds.), Deep-Water Reservoirs of The World. Gulf Coast Section SEPM 20th Bob F. Perkins Research Conference. 533-555.

Masalimova, L.U., Lowe, D.R., Sharman, G.R., King, P.R., Arnot, M.J., 2016. Outcrop characterization of a submarine channel-lobe complex: the lower Mount Messenger Formation, Taranaki Basin, New Zealand. Marine and Petroleum Geology 71, 360-390.

McHargue, T., Pyrcz, M.J., Sullivan, M.D., Clark, J.D., Fildani, A., Romans, B.W., Covault, J.A., Levy, M., Posamentier, H.W.,Drinkwater, N.J., 2011. Architecture of turbidite channel systems on the continental slope: patterns and predictions. Marine and Petroleum Geology 28, 728-743.

Métivier, F., Lajeunesse, E., Cacas, M.-C., 2005. Submarine canyons in the bathtub. Journal of Sedimentary Research 75, 6–11. doi: 10.2110/jsr.2005.002.

Migeon, S., Ducassou, E., Le Gonidec, Y., Rouillard, P., Mascle, J., Revel-Rolland, M., 2010. Lobe construction and sand/mud segregation by turbidity currents and debris flows on the western Nile deep-sea fan (Eastern Mediterranean). Sedimentary Geology 229, 124-143. doi:10.1016/j.sedgeo.2010.02.011.

Mulder, T., Etienne, S., 2010. Lobes in deep-sea turbidite systems: state of the art. Sedimentary Geology 229, 75–80, doi:10.1016/j.sedgeo.2010.06.011.

Mutti, E., 1977. Distinctive thin-bedded turbidite facies and related depositional environments in the Eocene Hecho Group (South-central Pyrenees, Spain). Sedimentology 24, 107-131.

Mutti, E., 1979. Turbidites et cones sous-marins profonds. In: P.Homewood (Ed.), Sedimentation Detritique (Fluviatile, Littorale et Marine). Institut Geologique Universite de Fribourg, Switzerland. 353-419.

Mutti, E., Ghibaudo, G., 1972. Un Esempio di torbiditi di conoide sottomarina esterna: le Arenarie di San Salvatore (formazione di Bobbio, Miocene) nell'Appennino di Piacenza: memoria di Emiliano Mutti e Guido Ghibaudo. Accademia delle scienze.

Mutti, E., Ricci Lucchi, F., 1972. Le torbiditi delt Apennino settentrionale: introduzione all’analisi di facies. Memorie Società. Geologica Italiana 11, 161–199.

Mutti, E., Sonnino, M., 1981. Compensation cycles: a diagnostic feature of turbidite sandstone lobes. International Association of Sedimentologists, 2nd European Regional Meeting, Bologna, Italy. 120–123.

Navarre, J.C., Claude, D., Liberelle, E., Safa, P., Vallon, G., Keskes, N., 2002. Deepwater turbidite system analysis, West Africa: Sedimentary model and implications for reservoir model construction. The Leading Edge 21, 1132-1139.

Normark, W. R., 1970. Growth patterns of deep sea fans. American Association of Petroleum Geologists Bulletin 54, 2170–2195.

Normark, W.R., 1978. Fan valleys, channels and depositional lobes on modern submarine fans: characteristics for recognition of sandy turbidite environments. American Association of Petroleum Geologists Bulletin 62, 912-931.

Normark, W.R., Posamentier, H., Mutti, E., 1993. Turbidite systems: state of the art and future directions. Reviews of Geophysics 31, 91-116.

O'Connell, S., Ryan, W. B., Normark, W. R., 1991. Evolution of a fan channel on the surface of the outer Mississippi Fan: evidence from side-looking sonar. P. Weimer, M.H. Link (Eds.), Seismic facies and sedimentary processes of submarine fans and turbidite systems. Springer, New York, 365-381.

Oluboyo, A.P., Gawthorpe, R.L., Bakke, K., Hadler-Jacobsen, F., 2014. Salt tectonic controls on deep-water turbidite depositional systems: Miocene, southwestern Lower Congo Basin, offshore Angola. Basin Research 26, 597-620.

Picot, M., Droz, L., Marsset, T., Dennielou, B., Bez, M., 2016. Controls on turbidite sedimentation: insights from a quantitative approach of submarine channel and lobe architecture (Late Quaternary Congo Fan). Marine and Petroleum Geology 72, 423-446.

Pierce, C.S., Haughton, P.D., Shannon, P.M., Pulham, A.J., Barker, S.P., Martinsen, O.J., 2018. Variable character and diverse origin of hybrid event beds in a sandy submarine fan system, Pennsylvanian Ross Sandstone Formation, western Ireland. Sedimentology 65, 952-992.

Pirmez, C., Beaubouef, R.T., Friedmann, S.J., Mohrig, D.C., 2000. Equilibrium profile and base level in submarine channels: examples from Late Pleistocene Systems and implications for the architecture of deepwater reservoir. In: Weimer, P., Slatt, R.M., Bouma, A.H., Lawrence, D.T., (Eds.), Deep-water reservoir of the world. Gulf Coast Section SEPM Foundation 20th Annual Research Conference. 782-805.

Posamentier, H.W., Meizarwin, P.S.W., Plawman, T., 2000. Deep water depositional systems—Ultra-deep Makassar Strait, Indonesia. In: Weimer, P., Slatt, R.M., Coleman, J., Rosen, N.C., Nelson, H., Bouma, A.H., Styzen, M.J., Lawrence, D.T., (Eds.), Deep-Water Reservoirs of the World: Gulf Coast Society of the Society of Economic Paleontologists and Mineralogists Foundation, 20th Annual Research Conference. 806–816.

Posamentier, H. W., Kolla, V., 2003. Seismic geomorphology and stratigraphy of depositional elements in deep-water settings. Journal of Sedimentary Research. 73, 367-388.

Prather, B.E., 2000. Calibration and visualization of depositional process models for above-grade slopes: a case study from the Gulf of Mexico. Marine and Petroleum Geology 17, 619–638.

Prather, B.E., 2003. Controls on reservoir distribution, architecture and stratigraphic trapping in slope settings. Marine and Petroleum Geology 20, 529–545.

Prather, B.E., Booth, J.R., Steffens, G.S., Craig, P.A., 1998. Classification, lithologic calibration and stratigraphic succession of seismic facies from intraslope basins, deep water Gulf of Mexico, U.S.A. American Association of Petroleum Geologists Bulletin 82, 701–728.

Prather, B.E., Pirmez, C., Sylvester, Z., Prather, D., 2012a. Stratigraphic response to evolving geomorphology in a submarine apron perched on the upper Niger Delta slope. In: Prather, B.E., Deptuck, M.E., Mohrig, D., Van Hoorn, B., Wynn, R.B., (Eds.), Application of the principles of seismic geomorphology to continental slope and base-of-slope systems: case studies from seafloor and near-seafloor analogues. SEPM Special Publication 99, 145–161.

Prather, B.E., Pirmez, C., Winker, C.D., Deptuck, M.E., Mohrig, D., 2012b. Stratigraphy of linked intraslope basins: Brazos-Trinity system western Gulf of Mexico. Application of the principles of seismic geomorphology to continental-slope and base-of-slope systems: Case studies from seafloor and near-seafloor analogues. SEPM, Special Publication, 99, 83-109.

Prélat, A., Hodgson, D.M., Flint, S.S., 2009. Evolution, architecture and hierarchy of distributary deep-water deposits: a high-resolution outcrop investigation from the Permian Karoo Basin, South Africa. Sedimentology 56, 2132-2154. doi: 10.1111/j.1365-3091.2009.01073.x

Prélat, A., Covault, J.A., Hodgson, D.M., Fildani, A., Flint, S.S., 2010. Intrinsic controls on the range of volumes, morphologies, and dimensions of submarine lobes. Sedimentary Geology 232, 658–674. doi:10.1016/j.sedgeo.2010.09.010.

Prélat, A., Hodgson, D.M., 2013. The full range of turbidite bed thickness patterns in submarine lobes: controls and implications. Journal of the Geological Society [London] 170, 209-214. doi: 10.1144/jgs2012-056.

Pyles, D.R., Jennette, D.C., 2009. Geometry and architectural associations of co-genetic debrite–turbidite beds in basin-margin strata, Carboniferous Ross Sandstone (Ireland): Applications to reservoirs located on the margins of structurally confined submarine fans. Marine and Petroleum Geology 26, 1974-1996.

Pyles, D.R., Strachan, L.J., Jennette, D.C., 2014. Lateral juxtapositions of channel and lobe elements in distributive submarine fans: Three-dimensional outcrop study of the Ross Sandstone and geometric model. Geosphere 10, 1104-1122.

Reading, H.G., Richards, M., 1994. Turbidite systems in deep-water basin margins classified by grain size and feeder system. American Association of Petroleum Geologists Bulletin 78, 792-822.

Remacha, E., Fernandez, L.P., Maestro, E., 2005, The transition between sheet-like lobe and basin-plain turbidites in the Hecho Basin (South-Central Pyrenees, Spain). Journal of Sedimentary Research 75, 798–819. doi: 10.2110/jsr.2005.064.

Rowland, J.C., Hilley, G.E., Fildani, A., 2010. A test of initiation of submarine leveed channels by deposition alone. Journal of Sedimentary Research 80, 710-727.

Ruzuar, A.P., Schneinder, R., Saller, A.H., Noah, J.T., 2005. Linked Lowstand Delta to Basin-Floor Fan Deposition, Offshore East Kalimantan: An Analogue for Deep-Water Reservoir Systems. Proceedings, Indonesian Petroleum Association Thirtieth Annual Convention and Exhibition, August 2005. 467-481.

Saller, A.H., Noah, J.T., Schneider, R., Ruzuar, A.P., 2003, December. Lowstand deltas and a basin-floor fan, Pleistocene, offshore East Kalimantan, Indonesia. In: Margin deltas and linked down slope petroleum systems: Global significance and future exploration potential. Gulf Coast Section SEPM Foundation 23rd Annual Bob F. Perkins Research Conference. 421-440.

Saller, A.H., Noah, J.T., Ruzuar, A.P., Schneider, R., 2004. Linked lowstand delta to basin-floor fan deposition, offshore Indonesia: An analog for deep-water reservoir systems. American Association of Petroleum Geologists Bulletin 88, 21-46.

Saller, A., Werner, K., Sugiaman, F., Cebastiant, A., May, R., Glenn, D., Barker, C., 2008, Characteristics of Pleistocene deep-water fan lobes and their application to an upper Miocene reservoir model, offshore East Kalimantan, Indonesia. American Association of Petroleum Geologists Bulletin 92, 919–949.

Saller, A.H., Dharmasamadhi, I.N.W., Lilburn, T., Earley, R., 2010. Seismic geomorphology of submarine slopes: channel levee complexes versus slope valleys and canyons, Pleistocene, East Kalimantan, Indonesia. In: Wood, Lesli J., Simo, Toni T., Rosen, Norman C. (Eds.), Seismic Imaging of Depositional and Geomorphic Systems. Gulf Coast Section SEPM, 30th Annual Conference. 433-471.

Shanmugam, G., Shrivastava, S.K., Das, B., 2009. Sandy debrites and tidalites of Pliocene reservoir sands in upper-slope canyon environments, offshore Krishna–Godavari Basin (India): implications. Journal of Sedimentary Research 79, 736-756.

So, Y.S., Rhee, C.W., Choi, P.Y., Kee, W.S., Seo, J.Y., Lee, E.J., 2013. Distal turbidite fan/lobe succession of the Late Paleozoic Taean Formation, western Korea. Geosciences Journal 17, 9-25. doi: 10.1007/s12303-013-0016-0.

Sprague, A.R., Sullivan, M.D., Campion, K.M., Jensen, G.N., Goulding, D.K., Sickafoose, D.K., Jennette, D.C., 2002. The physical stratigraphy of deep-water strata: a hierarchical approach to the analysis of genetically related elements for improved reservoir prediction. American Association of Petroleum Geologists Annual Meeting abstracts, Houston, Texas. 10-13.

Sprague, A.R.G., Garfield, T.R., Goulding, F.J., Beaubouef, R.T., Sullivan, M.D., Rossen, C., Campion, K.M., Sickafoose, D.K., Abreu, V., Schellpeper, M.E., Jensen, G.N., Jennette, D.C., Pirmez, C., Dixon, B.T., Ying, D., Ardill, J., Mohrig, D.C., Porter, M.L., Farrell, M.E., Mellere, D., 2005. Integrated slope channel depositional models: the key to successful prediction of reservoir presence and quality in offshore West Africa. CIPM, cuarto E-Exitep 2005, February 20-23, 2005, Veracruz, Mexico. 1-13.

Spychala, Y.T., Hodgson, D.M., Flint, S.S., Mountney, N.P., 2015. Constraining the sedimentology and stratigraphy of submarine intraslope lobe deposits using exhumed examples from the Karoo Basin, South Africa. Sedimentary Geology 322, 67-81. doi: 10.1016/j.sedgeo.2015.03.013.

Steffens, G.S., Biegert, E.K., Sumner, H.S., Bird, D., 2003. Quantitative bathymetric analyses of selected deepwater siliciclastic margins: receiving basin configurations for deepwater fan systems. Marine and Petroleum Geology. 20, 547-561.

Stow, D. A. V., 1985. Deep-sea clastics: where are we and where are we going? In: Brenchley, P. J., Williams, B. P. J., (Eds.), Sedimentology: recent developments and applied aspects. London, Geological Society [London] Special Publication 18, 67–93.

Stow, D. A. V., 1986. Deep clastic seas. In: Reading, H. G., ed., Sedimentary environments and facies. Oxford, Blackwell Scientific Publications. 399–444.

Straub, K.M., Pyles, D.R., 2012. Quantifying the hierarchical organization of compensation in submarine fans using surface statistics. Journal of Sedimentary Research 82, 889-898. doi: 10.2110/jsr.2012.73.

Sullivan, M.D., Jensen, G.N., Goulding, F.J., Jennette, D.C., Foreman, J.L., Stern, D., 2000. Architectural analysis of deep-water outcrops: Implications for exploration and production of the Diana Sub-basin, western Gulf of Mexico. In: Weimer, P., Slatt, R.M., Coleman, J., Rosen, N.C., Nelson, H., Bouma, A.H., Styzen, M.J., Lawrence, D.T. (Eds.), Deep-Water Reservoirs of The World. Gulf Coast Section SEPM 20th Bob F. Perkins Research Conference. 1010-1032.

Sylvester, Z., Deptuck, M.E., Prather, B.E., Pirmez, C., O'Byrn, C., 2012. Seismic stratigraphy of a shelf-edge delta and linked submarine channels in the northeastern Gulf of Mexico. In: Prather, B.E., Deptuck, M.E., Mohrig, D., Van Hoorn, B., Wynn, R.B. (Eds.), Application of the principles of seismic geomorphology to continental slope and base-of-slope systems: case studies from seafloor and near-seafloor analogues. SEPM Special Publication 99, 31-59.

Terlaky, V., Rocheleau, J., Arnott, R.W.C., 2016. Stratal composition and stratigraphic organization of stratal elements in an ancient deep-marine basin-floor succession, Neoproterozoic Windermere Supergroup, British Columbia, Canada. Sedimentology 63, 136-175. doi: 10.1111/sed.12222.

Twichell, D.C., Schwab, W.C., Nelson, H.C., Kenyon, N.H., Lee, H.J., 1992, Characteristics of a sandy depositional lobe on the outer Mississippi Fan from SeaMARC IA Sidescan Sonar images. Geology 20, 689–692.

Twichell, D., Nelson, C.H., Kenyon, N., Schwab, W., 2009. The influence of external processes on the Holocene evolution of the Mississippi Fan. In: Kneller, B., Martinsen, O.J., McCaffrey, W.D. (Eds.), External Controls on Deepwater Depositional Systems. SEPM Special Publication 92, 145-157.

Van der Merwe, W.C., Hodgson, D.M., Brunt, R.L., Flint, S.S., 2014. Depositional architecture of sand-attached and sand-detached channel-lobe transition zones on an exhumed stepped slope mapped over a 2500 km^2 area. Geosphere. 10, 1076-1093. doi:10.1130/GES01035.

Walker, R. G., 1978. Deep-water sandstone facies and ancient submarine fans: models for exploration for stratigraphic traps. American Association of Petroleum Geologists Bulletin 62, 932–966.

Weimer, P., Slatt, R.M., Coleman, J., Rossen, N.C., Nelson, H., Bouma, A.H., Styzen, M.J., Lawrence, D.T. (Eds.), 2000. Deep-water reservoirs of the world. Gulf Coast Section SEPM Foundation 20th Annual Research Conference.

Yang, Su-Yeong, Kim, Jae Woo, 2014. Pliocene basin-floor fan sedimentation in the Bay of Bengal (offshore northwest Myanmar). Marine and Petroleum Geology 49, 45-58.

FIGURE CAPTIONS:

Figure 1. An RMS (root mean squared) amplitude extraction of Lobate Example 1 from a 3D reflection seismic volume on the middle slope, off shore Nigeria. The image is calculated from the interval between 10ms and 20ms from the top of the lobate deposit (see Figure 2). High RMS values are displayed as white to yellow colors. Modified from Prélat et al. (2010).

Figure 2. Cross sections through Lobate Example 1 from a 3D reflection seismic volume. (A) Plan view RMS (root mean squared) amplitude extraction midway between the upper and lower bounding surfaces of Lobate Example 1 (blue horizons in figures B-E) superimposed on a

coherency display (lateral rate of change of amplitude values from the same interval). High RMS values are displayed as white to yellow colors. Low coherency values are displayed in black. Modified from Prélat et al. (2010). The locations of cross-sections B-E are displayed as red lines. (B) Proximal section through the feeder channel complex for Lobate Example 1. Prominent levees are present on both sides of the channel complex. (C) Seismic section through the proximal portion of Lobate Example 1. This portion of the lobate deposit is characterized by highly discontinuous reflections resulting from the presence of numerous distributary channels. The top of a single lens-shaped unit is highlighted as a yellow horizon. (D) Seismic section through the medial portion of Lobate Example 1. This portion of the lobate deposit is characterized by moderately discontinuous reflections, resulting from the presence of numerous distributary channels. The top of one lens-shaped unit is highlighted as a yellow horizon. (E) Seismic section through the distal portion of Lobate Example 1. This portion of the lobate deposit is characterized by moderately continuous reflections. Very small distributary channels appear to be present in plan view but are too shallow to break up reflection continuity in section view. The top of a single lens-shaped unit is highlighted as a yellow horizon.

Figure 3. An RMS (root mean squared) amplitude extraction from two adjacent 3D reflection seismic volumes on the middle to upper slope, off shore Nigeria. The image is calculated from the interval between 50 and 150 milliseconds (approximately 85m of sediment) below seabed. Water Depth increases to the southwest. High RMS values are displayed as white to orange colors. The approximate position of the shelf edge is represented by a red dashed line. The boarders of large slump complexes at the shelf edge are indicated by scallop-shaped indentations in the shelf edge. The boarders of a large slump scar complex on the upper slope are indicated

by an orange dashed line. The location of Lobate Example 2 is labeled as are the locations of areas X and Y (discussed in the text).

Figure 4. An RMS (root mean squared) amplitude extraction from two adjacent 3D reflection seismic volumes on the middle to upper slope, off shore Nigeria. See Figure 3 for location. The image is calculated from the interval between 50 and 150 milliseconds (approximately 85m of sediment) below seabed. Water Depth increases to the southwest. High RMS values are displayed as white to orange colors. The location of Lobate Example 2 is labeled, as are the locations of areas Y, and Z (discussed in the text).

Figure 5. An RMS (root mean squared) amplitude extraction from a 3D reflection seismic volume of Lobate Example 2 on the middle slope, off shore Nigeria. See Figures 3 and 4 for location. The image is calculated from the interval between 50 and 100 milliseconds (approximately 43m of sediment) below seabed. The sampled interval is indicated by the interval between blue lines in Figure 6. Water Depth increases to the southwest. High RMS values are displayed as white to yellow colors. The locations of seismic cross sections in Figure 6 are indicated by yellow lines labeled A, B, and C.

Figure 6. Cross sections through Lobate Example 2 from a 3D reflection seismic volume. See Figure 5 for locations. The blue lines indicate the top and base of the interval from which the RMS (root mean squared) values in Figure 5 were calculated. (A) Seismic section through the distal portion of Lobate Example 2. This portion of the lobate deposit is characterized by highly continuous reflections. Incisional bypass channels are evident to the west of Lobate Example 2. (B) Seismic section through the terminus of Lobate Example 2. The lobate deposit continues to be characterized by highly continuous reflections. The area to the west of Lobate Example 2 is

dominated by multiple incisional bypass channels. (C) Seismic section across a highly incisional channel that exits the perched basin through the saddle between structural highs. Presumably, multiple flow pathways are funneled through this erosional fairway providing sand-rich sediments farther down slope.

Figure 7. An RMS (root mean squared) amplitude extraction of Lobate Example 3 from a 3D reflection seismic volume at the base of slope, Kutei Basin, off shore Kalimantan, Indonesia. The image is horizon referenced and derived from the interval 0-50ms above the base of the lobate deposit (purple horizon in Figure 8). High RMS values are displayed as white color. Modified from Posamenier et al. (2000), Fowler et al. (2001), Posamentier and Kolla (2003), Saller et al. (2003, 2004, 2008 and 2010), and Ruzuar et al. (2005).

Figure 8. Cross sections through Lobate Example 3 from a 3D reflection seismic volume. See Figure 7 for locations. The green and purple horizons indicate the top and base respectively of Lobate Example 3 (highlighted in yellow). (A) Seismic section through the feeder channel complex of Lobate Example 3. (B) Seismic section through the proximal part of Lobate Example 3. (C) Seismic section through the distal part of Lobate Example 3.

Figure 9. Summary of distinctive characteristics of the three discussed lobate examples. See Figures 1, 5, and 7 for explanations of seismic RMS amplitude displays.

Figure 10. Generalized illustrations of the three models of lobate deposits proposed here emphasizing their distinctive characteristics. (A) Pervasively channelized. (B) Unchannelized. (C) Few long, straight distributaries.

Figure 11. Hill-shade maps based on LiDAR produced topography of subaerial fans with contrasting distributary patterns. (A) Debris flow dominated fan in Saline Valley, California. Laminar flow of the subaerial debris flows has produced a surface distributary texture with long, nearly straight channels, sparse avulsion nodes, and narrow depositional bodies. This distributive architecture is reminiscent of Lobate Example 3 (Figure 7). Source: Earthscope Eastern and Southern California. Resolution = 0.5m. Lat. 36.824674°, Long. -117.919470°. (B) Alluvial fan in Death Valley, California, sculpted by turbulent runoff during infrequent heavy rains. The surface of the fan displays a pervasive distributary texture with low sinuosity flow paths and frequent avulsion nodes reminiscent of Lobate Example 1(Figure 1). Source: NCALM dataset for Death Valley. Resolution = 1m. Lat. 36.893189°, Long. -117.270879°. The material for both examples is based on services provided to the Plate Boundary Observatory by NCALM (http://www.ncalm.org). The Plate Boundary Observatory is operated by UNAVCO for EarthScope (http://www.earthscope.org) and supported by the National Science Foundation (No. EAR-0350028 and EAR-0732947).

Table 1. Tabular summary of contextual data and observations associated with each of the three discussed lobate examples.

Table 1

	Lobate Examples		
	1	2	3
Water Depth	2250m	1275m	2000m
Burial Thickness	120m	47m	160m
Seismic Dominant	60Hz	60Hz	50Hz
Seismic Resolution	15m	15m	17m
Sediment Source	Major Delta	Major Delta	Major Delta
Sediment Delivery	Large Leveed Channel Complex	From Littoral Drift Via Multiple Small Non-leveed Gullies	Large Erosional Channel Complex
Depositional Setting	Mid Slope	Mid Slope	Base of Slope
Length (L)	12km	14km	7 km
Width (W)	14km	6km	7 km
Maximum Thickness (T)	130m	20m	43m
Aspect Ratio (W/T)	108/1	300/1	163/1
Avulsion Nodes	Pervasive	0	1
Distributary number	Pervasive	0	Few (~5)
Surface Texture	Channelized	Smooth With Scours	Nodular to Smooth
Dominant Process	Turbulent Stratified Flows with Thick Dilute Layer	Collapse of Turbulent Stratified Flows with Thin Dilute Layer	Debris Flows Abundant to Dominant

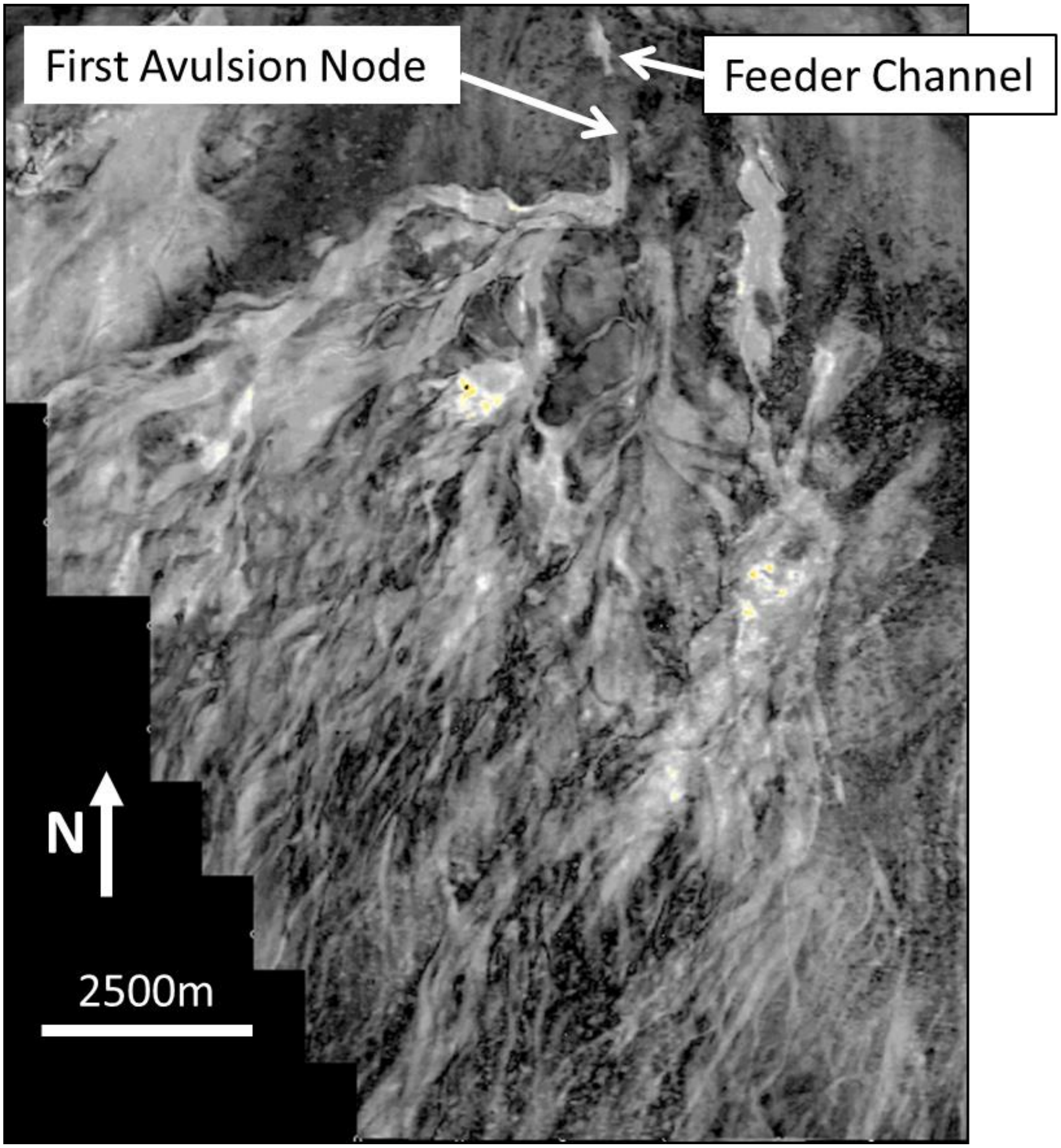

Figure 1

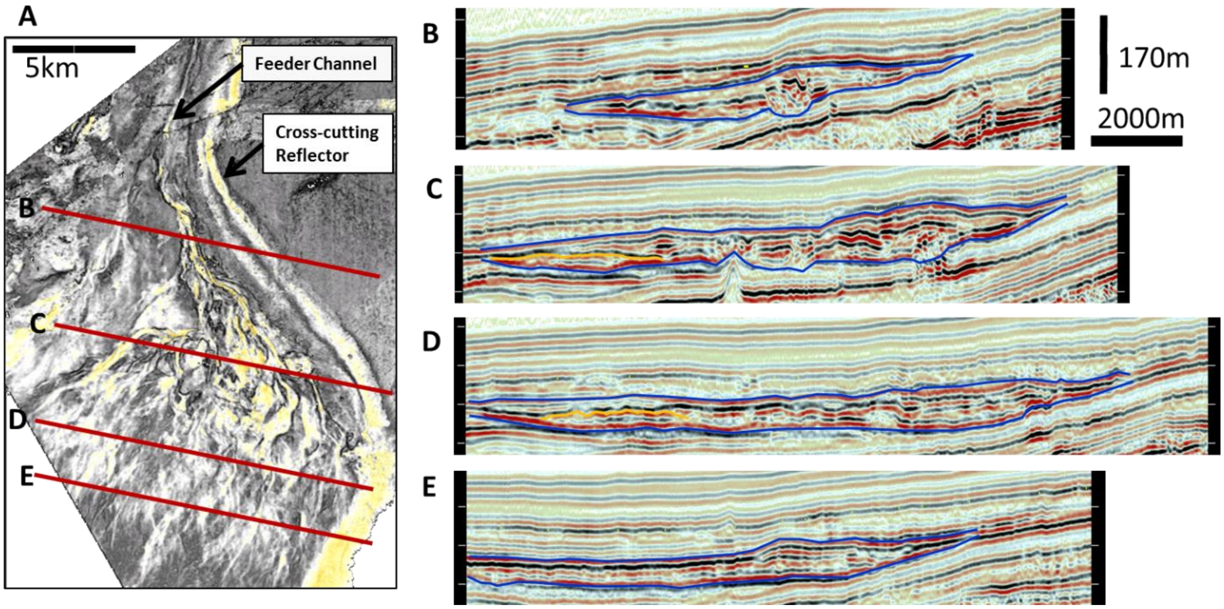

Figure 2

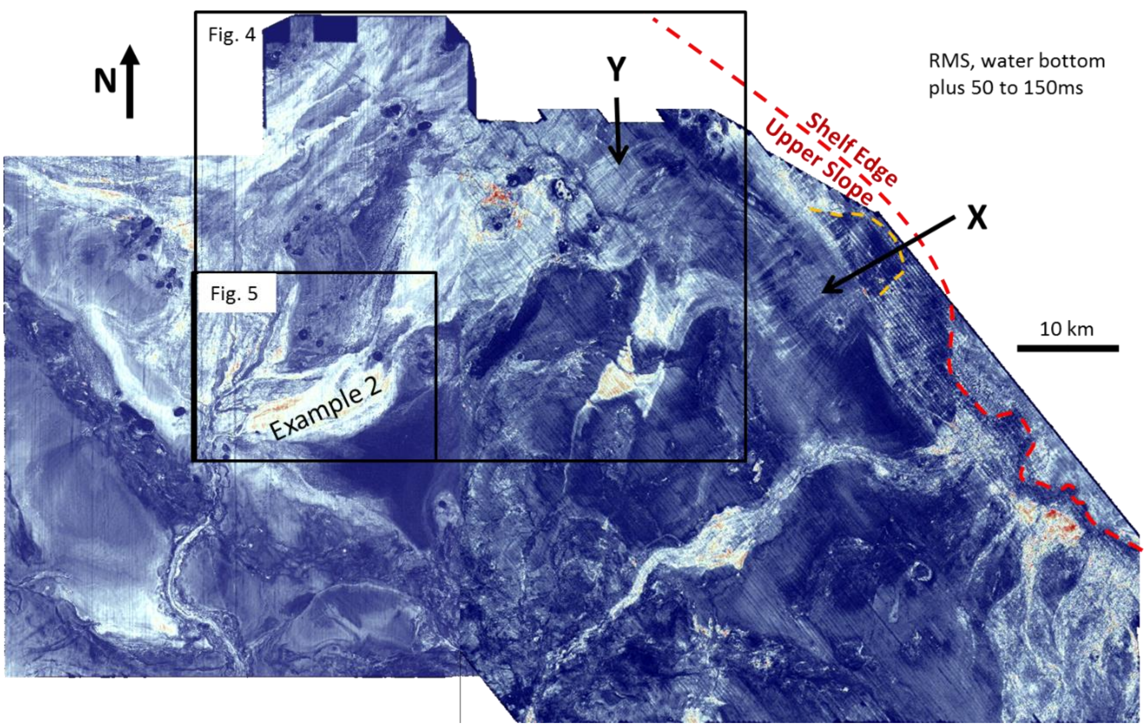

Figure 3

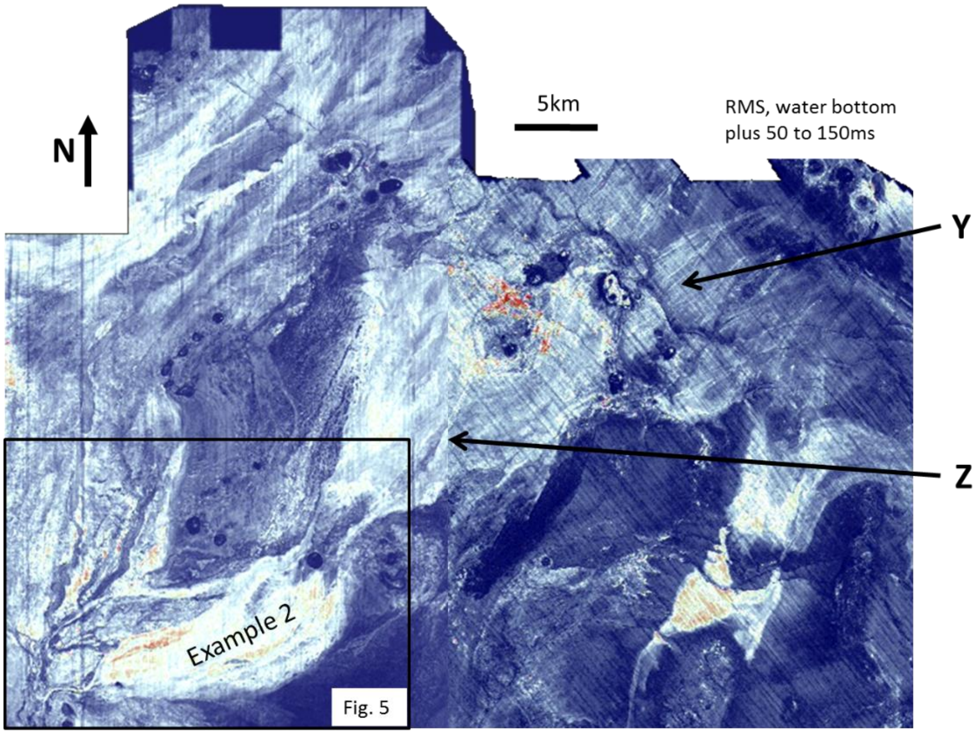

Figure 4

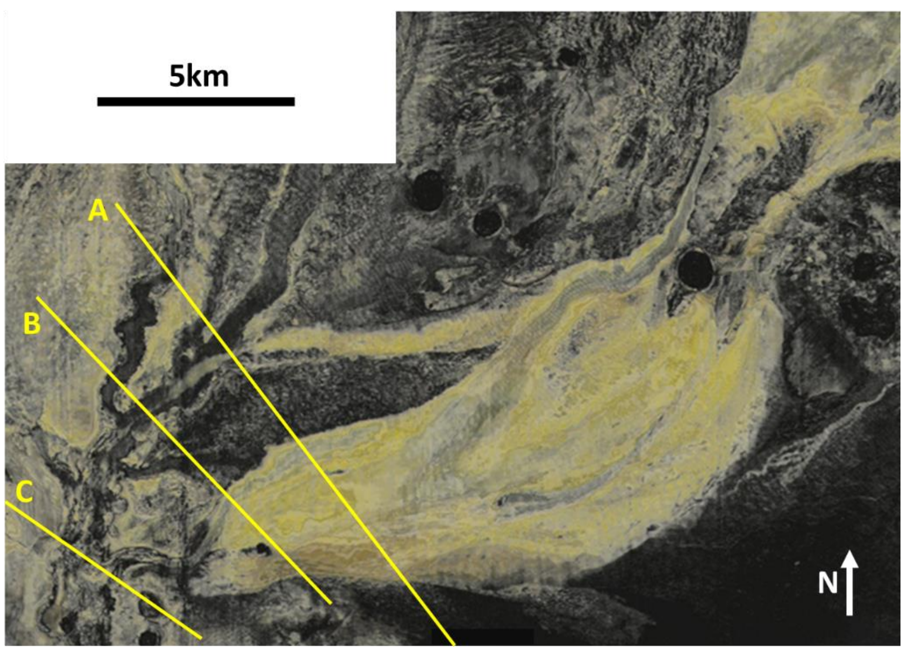

Figure 5

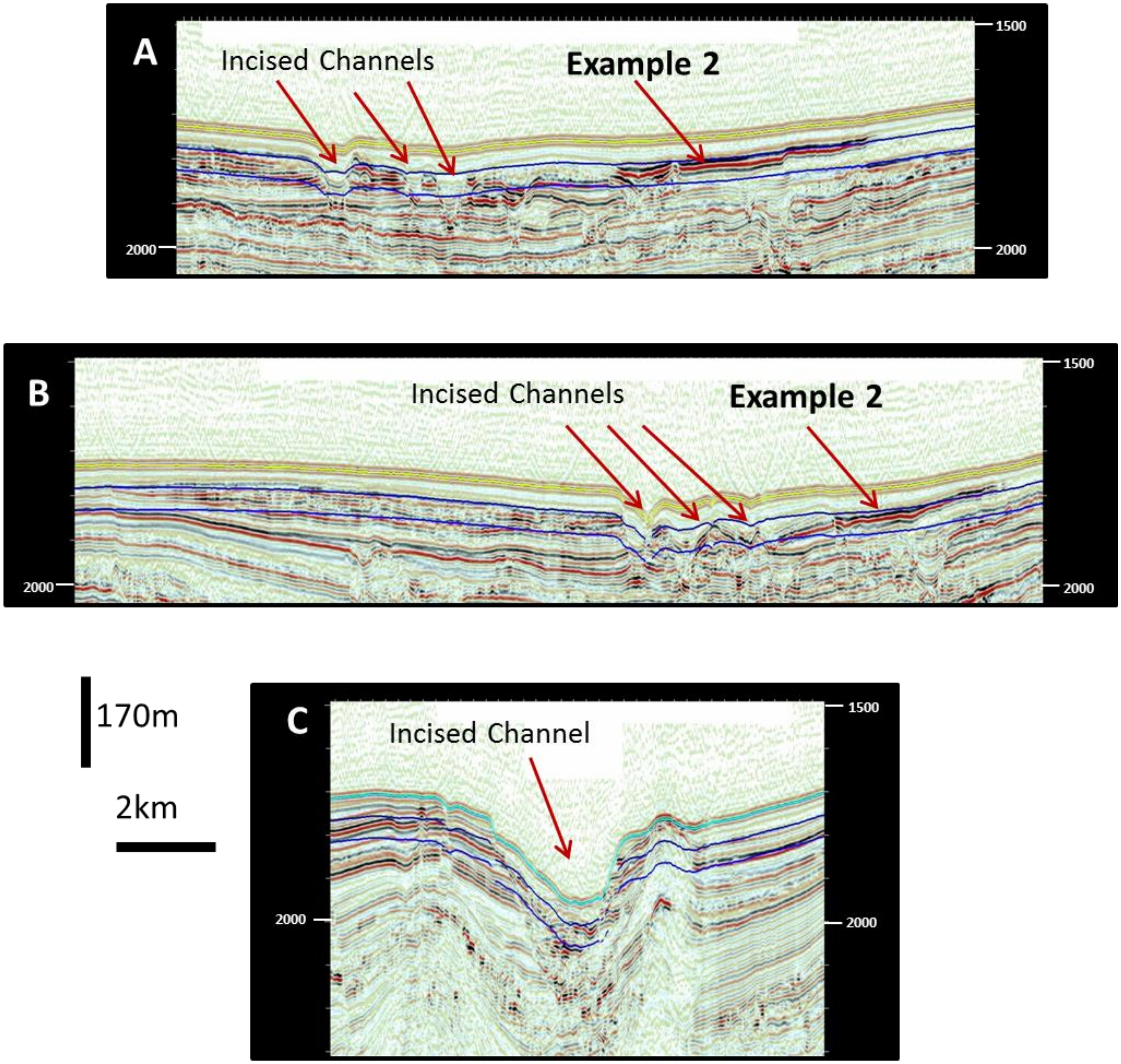
A
Incised Channels
Example 2
1500
2000
2000
B
Incised Channels
Example 2
1500
2000
2000
170m
2km
C
Incised Channel
1500
2000
2000

Figure 6

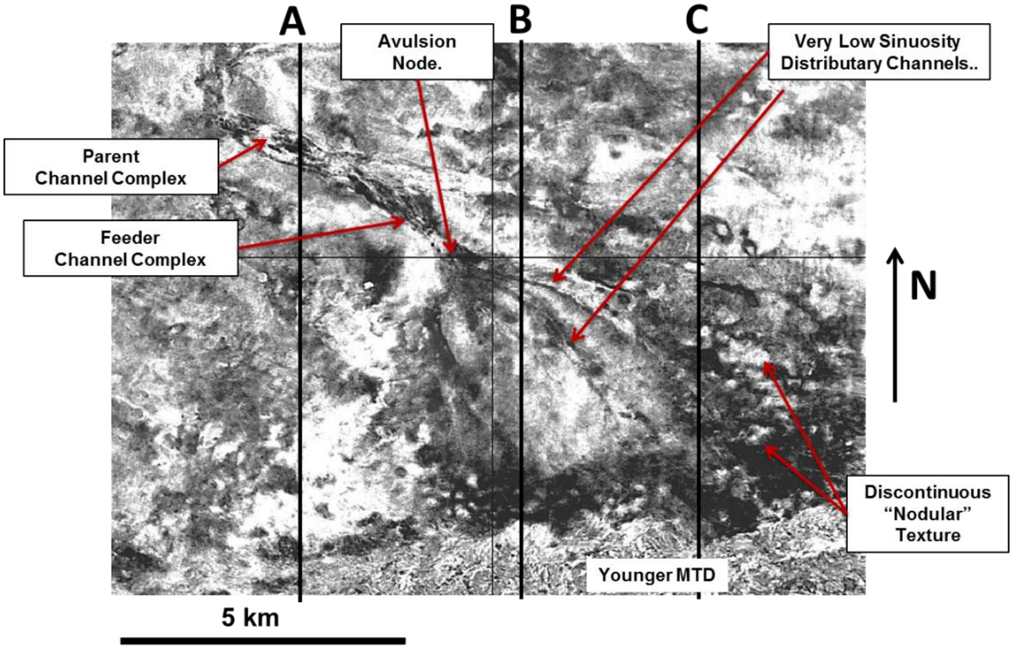

Figure 7

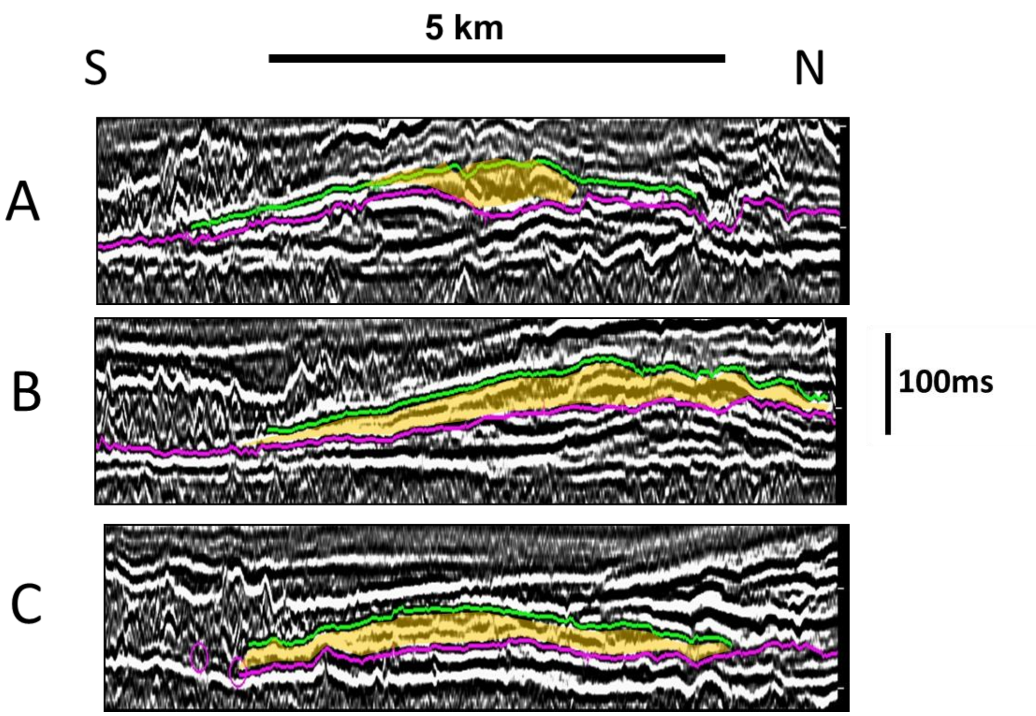

Figure 8

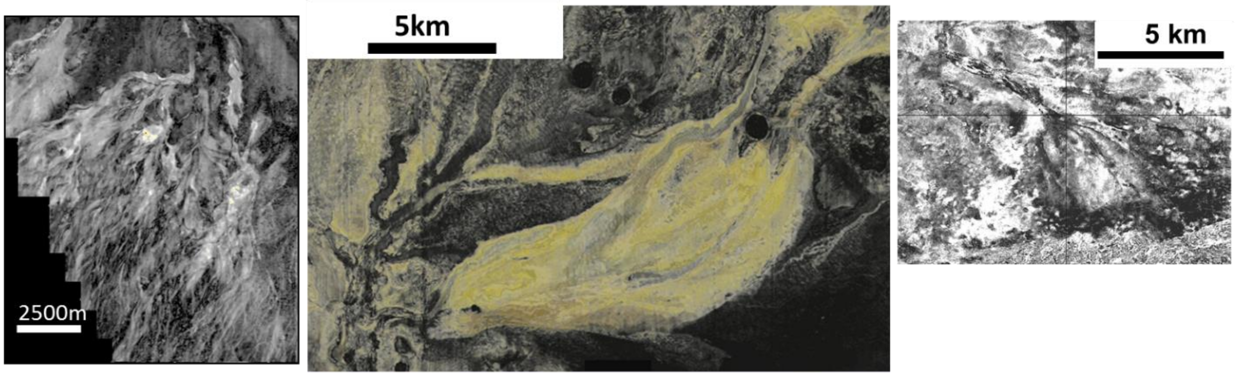

1: Pervasively channelized

- Mud-rich stratified flows
- Single levee-confined feeder channel
- Extensive system of distributary channels
- Proximal distributaries are levee confined
- Numerous avulsion nodes
- Aspect ratio = 108/1

2: Unchannelized

- Mud-poor stratified flows
- Fed by littoral drift
- Transport via multiple erosional gullies and channels
- Feeder channels lack any resolvable levees
- Elongate scours with non-parallel sides
- Deposition results from flow collapse
- Aspect ratio = 300/1

3: Few long, straight distributaries

- Debris flow dominated
- Straight, erosional feeder channel
- Nodular" seismic character represents rafted blocks
- Rare avulsions, mostly at the mouth of the feeder channel
- Aspect ratio = 163/1

Figure 9

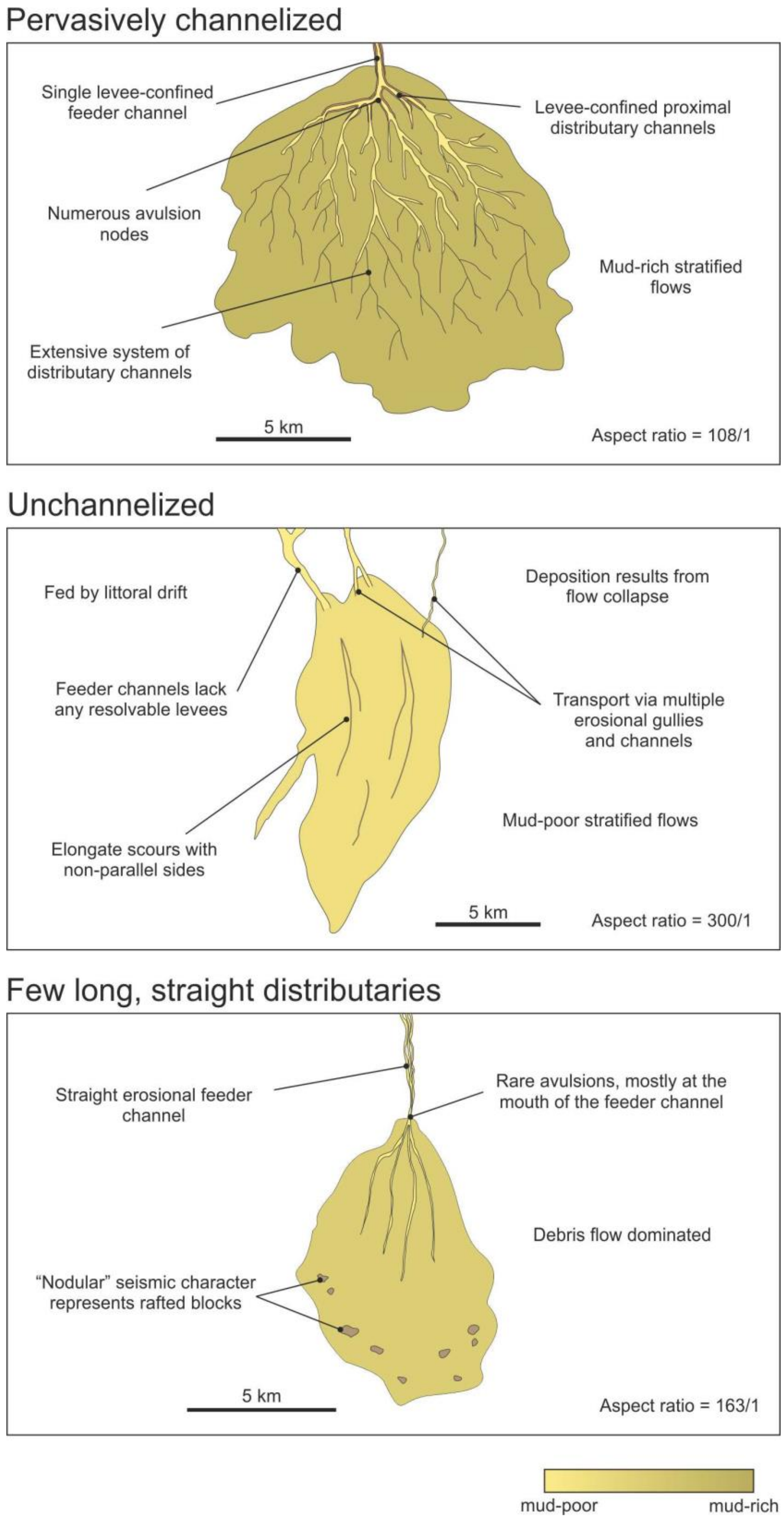

1523

1524 Figure 10

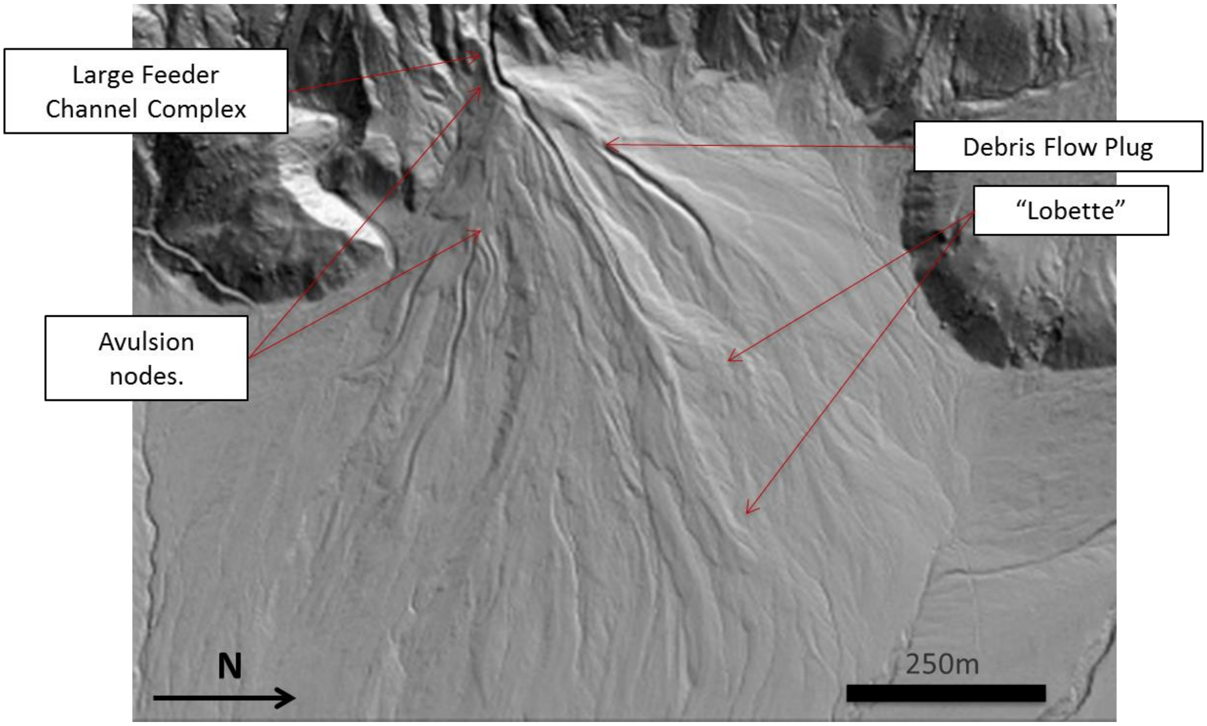
Large Feeder Channel Complex
Debris Flow Plug
"Lobette"
Avulsion nodes.
N
250m

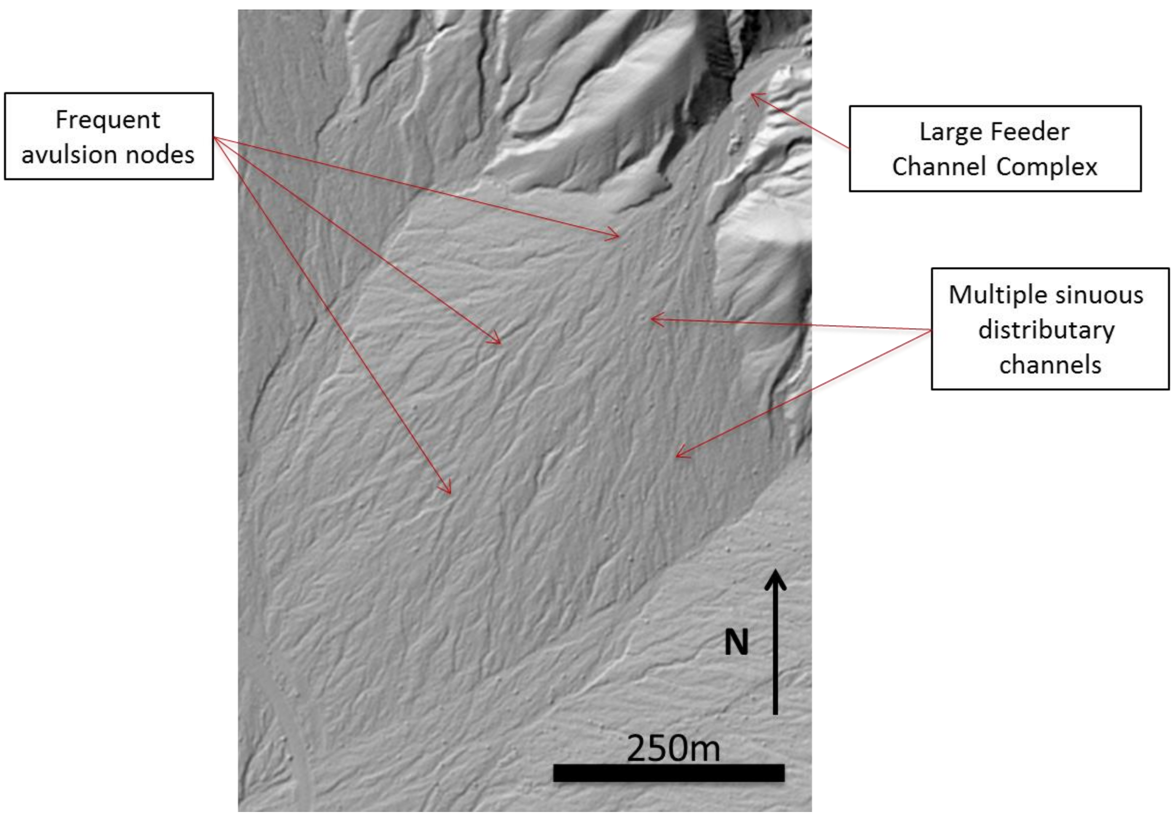
Frequent avulsion nodes
Large Feeder Channel Complex
Multiple sinuous distributary channels
N
250m

Figure 11